Chapter 2

HYDROGEN GENERATION BY WATER SPLITTING

2.1 Introduction

While today hydrogen is predominately generated from the processing of fossil fuels, which as a by-product results in the release of CO_2, this does us no good within the scheme of trying to prevent catastrophic global warming, nor any good within the less-immediate but still real issue of fossil fuel depletion. This chapter briefly discusses avenues to hydrogen production (other than photoelectrolysis) by splitting of the water molecule to generate hydrogen and oxygen that do not, necessarily, result in the emission of climate-altering gases.

The 1973 oil embargo motivated significant research efforts in hydrogen production [1-4] that were subsequently abandoned when the fossil fuel flood-gates were re-opened. Recently emerging concerns over energy security, and the maintenance of our global ecosystem has rekindled the search for the processes that are efficient, economical and practical for large-scale production of hydrogen; herein we consider some possibilities.

2.2 Hydrogen Production By Water Electrolysis

Electrolysis of water to generate hydrogen and oxygen has a history of more than 200 years [5]. It is the simplest of all the water-splitting techniques and comparatively efficient. The net reaction is

$$H_2O \text{ (liquid/vapor)} + \text{electrical energy} \rightarrow H_2 \text{ (g)} + \tfrac{1}{2} O_2 \text{ (g)} \quad (2.2.1)$$

Oxygen, a highly useful gas, is the only by-product. Water electrolyzers today satisfy approximately 3.9% of the world's

hydrogen demand [6]. Electrolyzers are used to produce hydrogen at levels ranging from a few cm^3/min to several thousand m^3/hour, with units ranging in physical size from portable to essentially immovable [4,7,8]. Electrolyzers generally use electricity from the power grid, which in turn is predominately powered by the combustion of coal, resulting in expensive and eco-hostile operation [9]. For sustained development the electrolyzers will need to be run using electrical energy derived from renewable sources such as windmills or solar cells.

At standard ambient temperature and pressure, the change in Gibb's free energy ΔG for the water splitting reaction (2.2.1) is positive and hence the reaction is non-spontaneous; for the reaction to occur the electrical energy equivalent to the change in the Gibb's free energy ΔG of the reaction must be supplied. In an electrolytic cell the electrical energy is supplied by applying a potential difference between two electrodes placed in an electrolyte. Electrical energy to chemical energy conversion takes place at the electrode-solution interface through charge transfer reactions. A potential difference V applied between the electrodes can be used to do maximum work of nFV, where F is the Faraday constant and n is the number of moles of electrons involved in the reaction. If V_{rev} is the minimum voltage needed to drive the water splitting reaction,

$$\Delta G = nFV_{rev} \tag{2.2.2}$$

This is the maximum amount of useful work that can be derived from the system on driving the reaction in the opposite direction. Thus, V_{rev} corresponds to the reversible work and is consequently called the thermodynamic reversible potential. At 25°C and 1 bar, the ΔG for the water-splitting reaction is 237.178 kJ/mol [10]. Therefore,

$$V_{rev} = \Delta G/nF = 1.229V \tag{2.2.3}$$

The reaction at this voltage is endothermic and hence at isothermal conditions heat energy (=$T\Delta S$, where is S is entropy and T is the absolute temperature) must be absorbed from the surrounding environment for the increase in entropy associated with water

dissociation. On operating an electrolytic cell above V_{rev} heat is generated due to the losses in the cell and a fraction of this provides the additional energy needed for the entropy change.

When energy exactly equal to the enthalpy $\Delta H = \Delta G + T\Delta S$ (=285.83 kJ/mol at 1 bar and 25°C) for water splitting is supplied, no heat is absorbed or evolved by the system [10]. The voltage corresponding to this condition, the thermoneutral voltage V_{tn} is given by

$$V_{tn} = \Delta H/nF = 1.482 \text{ V} \tag{2.2.4}$$

At V_{tn} the electrolysis generates enough heat to compensate for $T\Delta S$. When the cell is operated above $V_{tn,}$ the reaction becomes exothermic and heat must be removed from the electrolytic cell for isothermal operation. However energy losses, associated with reaction kinetics as well as charge transport through electrical leads and the electrolyte, necessitate electrolyzer operation in this voltage regime. In the case of practical devices the operating voltage can be expressed as

$$V_{op} = V_{rev} + \eta_a + |\eta_c| + \eta_\Omega \tag{2.2.5}$$

where η_a and η_c are the anodic and cathodic overpotentials associated with the reaction kinetics (electrode polarization effects) and η_Ω is the Ohmic overpotential that arises due to the resistive losses in the cell [7].

The overvoltage represents the voltage in excess of the thermodynamic voltage, required to overcome the losses in the cell and obtain the desired output in terms of current density or amount of hydrogen from the cell. Slow electrode/electrolyte reactions and large resistive losses result in high overpotentials. The overpotentials should be reduced to increase the optimum current density. The electrode, both anodic and cathodic, overpotential arises as a result of several polarization effects. These include low activity of the electrodes in the electrolyte (known as activation overpotential) leading to slow-charge transfer processes and ion deficiency at the electrode surface for charge transfer to take place due to the poor mass transport through diffusion (diffusion overpotential), migration

or convection [7,11,12]. The electrode overpotential increases logarithmically with current density as given by the Tafel relation [13]

$$\eta = a + b \log (j) \tag{2.2.6}$$

where j is the current density and 'a' and 'b' are characteristic constants for the electrode system. The constant 'a' provides information about the electrocatalytic activity of the electrodes, and 'b' the slope of the Tafel plot (η Vs log j) carries information regarding the electrode reaction mechanisms. The electrode overpotential can be minimized by selecting electrode materials with high electrocatalytic activity, and maximum real to apparent surface area [14]. The Ohmic overvoltage is a consequence of the resistive losses in the cell that occur mainly at the electrodes, electrical lead wires, metal-metal joints, and inside the electrolyte. Reduction in the electrode separation and electrolyte-resistance lowers the Ohmic overvoltage [4,7,15]. Bubble formation by the product gases is also a source of activation and Ohmic overpotentials [15-18]. An increase in operating temperature helps to reduce both activation and Ohmic overvoltages as it enhances the reaction rate and reduces the electrolyte resistance. Overvoltage minimization is essential for high efficiency operation of the electrolytic cells.

The efficiency of water electrolysis is defined as ratio of the energy content of hydrogen (the energy that can be recovered by reoxidation of the hydrogen and oxygen to water) to the electrical energy supplied to the electrolyzer [19,20]. In terms of voltage, the efficiency can be expressed as

$$\varepsilon = V_{tn}/V_{op} \tag{2.2.7}$$

Ideally, a cell operating at V_{tn} can produce hydrogen at 100% thermal efficiency. The energy in excess of ΔG need not be supplied in the form of electrical energy, hence a voltage as low as V_{rev} can also be used to split water if the system is allowed to absorb heat from its surroundings. The operation is called allothermal operation. The cell is about 120% voltage efficient when the operating voltage is V_{rev}. This means that the fuel value of the hydrogen produced will be 120% of the heating value of the electrical energy input at this

operating condition [21]. When a cell is operated above V_{tn} heat generated inside the cell due to losses supply the extra energy needed for driving the water splitting reaction, a process called autothermal operation. The cells should be operated at low voltages and high current densities to achieve high efficiencies and high hydrogen production rates. Practical efficiencies lie in the range 50 to 90% [22].

The cell voltage V_{op} is largely decided by the operating temperature and pressure. The thermodynamic voltage for water splitting (V_{rev}) reduces with an increase in operating temperature as given by the relation [23,24] for °K.

$$V^0_{rev,\,T} = 1.5184 - 1.5421 * 10^{-3} * T + 9.523 * 10^{-5} * T * \ln T + 9.84 * 10^{-8} * T^2 \quad (2.2.8)$$

V_{rev} takes a value of 1.18V at 80°C. The over-voltages are lowered considerably at elevated temperatures due to the increased conductivity of the electrolyte and higher electrode activities. The reduction in thermodynamic voltage as well as over-voltages at elevated temperatures lower the operating voltage of the electrolytic cell, thereby increasing the water splitting efficiency with resultant energy savings. When temperature and pressure effects are considered it is accurate to use V_{HHV}, which is the higher heating value voltage, in place of V_{tn} for efficiency calculation [24]. V_{HHV} corresponds to the heat content of the dry product gases with respect to the liquid water at 25°C. Therefore,

$$\varepsilon = V_{HHV}/V_{op} \quad (2.2.9)$$

The absolute temperature dependence of V_{HHV} can be given by the relation [7,24].

$$V^0_{HHV,T} = 1.4146 + 2.205 * 10^{-4} * T + 1.0 * 10^{-8}\, T^2 \quad (2.2.10)$$

V_{HHV} increases slightly with temperature taking a value 1.494 V at 80°C.

The reversible voltage V_{rev} is related to the operating pressure as

$$V_{rev,T,P} = V^0_{rev,T} + (RT/2F) \ln [(P-P_w)^{1.5}/(P_w/P^0_w)] \qquad (2.2.11)$$

where R is the universal gas constant, F is Faraday constant, P is operating pressure of the electrolyzer and P_w and P^0_w are, respectively, the partial pressures of water vapor over the electrolyte and over pure water [23]. An increase in pressure raises the reversible voltage at the rate of ~ 43 mV for every ten-fold increase in pressure where it has only a negligible effect on V_{HHV} [4,18,23-25]. The over-voltages are considerably reduced at higher pressures and the savings in energy due to this is considered higher than the extra energy needed to overcome the theoretical voltage. Noted advantages of operation at higher pressures are: (1) higher optimum current density compared to the lower pressure cells operating at the same voltage; (2) enabling of higher operating temperatures; (3) suppression of bubble formation at high current densities; (4) elimination of equipment and its energy used for pressurizing the hydrogen as needed for practical applications; (5) prevention of water loss by evaporation from cells operating above 80°C [15,25]. However a recent analysis shows higher overall electrical energy consumption in pressurized electrolyzers compared to those operating at atmospheric pressure [18]. Furthermore problems such as corrosion, hydrogen embrittlement and other instabilities in the cell components are worse in pressurized electrolyzers. A source of inefficiency and purity loss in high-pressure electrolysis is the recombination of hydrogen and oxygen dissolved in the electrolyte that crosses over, respectively, into the anode and cathode compartments of the cell.

For hydrogen production from water, pure water (pH=7.0) is seldom used as an electrolyte. Water is a poor ionic conductor and hence it presents a high Ohmic overpotential. For the water splitting reaction to proceed at a realistically acceptable cell voltage the conductivity of the water is necessarily increased by the addition of acids or alkalis. Aqueous acidic and alkaline media offer high ionic (hydrogen and hydroxyl) concentrations and mobilities and therefore possess low electrical resistance. Basic electrolytes are generally preferred since corrosion problems are severe with acidic electrolytes. Based on the type of electrolytes used electrolyzers are

generally classified as alkaline, solid polymer electrolyte (SPE), and solid oxide electrolyte (SOE) which we now consider further.

Alkaline Electrolyzers

As the name indicates alkaline electrolyzers use high pH electrolytes like aqueous sodium hydroxide or potassium hydroxide. This is the oldest, most developed and most widely used method of water electrolysis. Hydrogen evolution takes place at the cathode, and oxygen evolution takes place at the anode. The cathodic reaction can be represented by the following steps [26,27]

$$H_2O + M + e^- \rightarrow M\text{-}H + OH^- \quad (2.2.12)$$
$$H_2O + M\text{-}H + e^- \rightarrow H_2 + M + OH^- \quad (2.2.13)$$
$$2M\text{-}H \rightarrow H_2 + 2M \quad (2.2.14)$$

M-H represents the hydrogen adsorbed at the active sites on the electrode surface. The hydrogen is first adsorbed onto the active sites on the cathode surface (reaction 2.2.12). Under the catalytic action of the electrode surface, the adsorbed hydrogen atoms combine together to form hydrogen molecules (reaction 2.2.13 and/or reaction 2.2.14). These molecules accumulate until a bubble forms which breaks away and rises to the electrolyte surface. The hydroxyl ions are discharged at the anode leading to oxygen evolution. The process can be represented as [28]

$$OH^- + M \rightarrow M\text{-}OH + e^- \quad (2.2.15)$$
$$M\text{-}OH + OH^- \rightarrow M\text{-}O + H_2O + e^- \quad (2.2.16)$$
$$2M\text{-}O \rightarrow O_2 + 2M \quad (2.2.17)$$

An alkaline electrolyzer consists mainly of a cell frame, electrolyte, anode, cathode and a separator [29]. A two-cell configuration is shown in **Figure 2.1.** The cell frame is generally made of stainless steel. The electrolyte should provide high ion conductivity, should not suffer chemical decomposition on the application of voltage so as to restrict the process to splitting of water molecules, and be capable of withstanding pH changes during the process as a result of the rapid changes in hydrogen ion

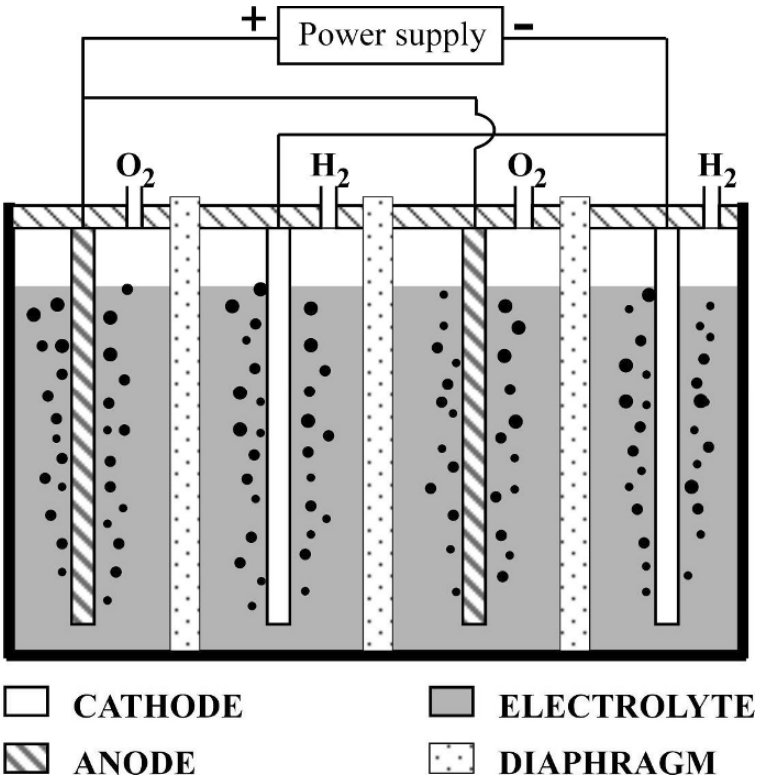

Fig. 2.1: Two-cell conventional alkaline electrolyzer configuration.

concentration at the electrodes. As acidic electrolytes cause corrosion problems, strong bases such as NaOH or KOH are commonly used as electrolytes [4,7]. The conductivity of the aqueous KOH is maximum when its concentration is near 28% and hence most of the electrolyzers use a concentration of 25% to 35% KOH in water [30]. The conductivity of this electrolyte decreases with increasing temperature reaching a maximum at approximately 150°C [7]. The electrolyte is circulated through cells, heat exchangers and filters to maintain a constant operating temperature, reduce polarization effects due to bubble formation and concentration gradients, and remove suspended solids and possible corrosion products. The electrolyte concentration is maintained by addition of high purity water as needed depending upon the hydrogen production rate. A schematic of an electrolyzer unit is

given in **Fig. 2.2**. The evolved hydrogen and oxygen vapor also contain that of the electrolyte, hence the vapors are initially passed through electrolyte-gas separators for purification; the hydrogen gas is then dried by passing through a condenser.

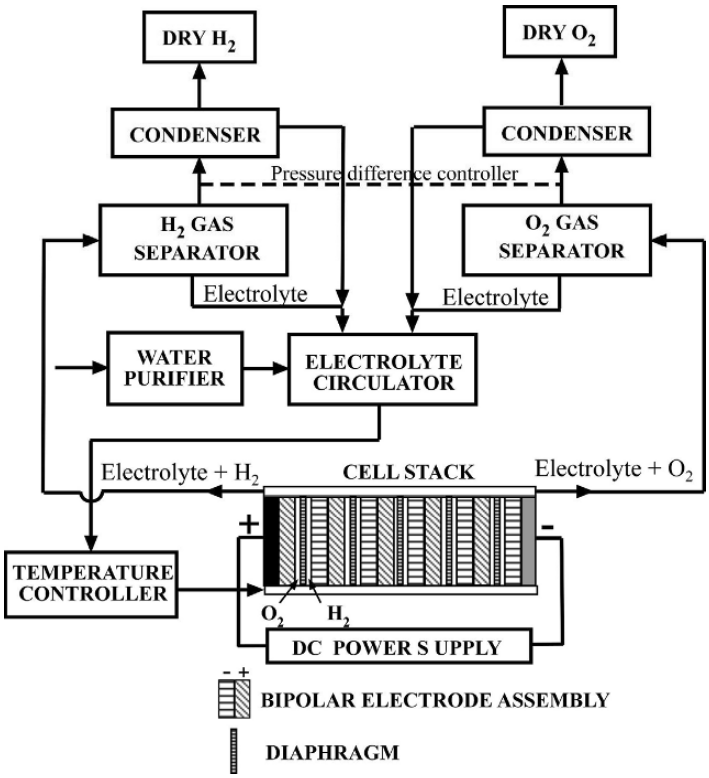

Fig. 2.2: Schematics of hydrogen production using an alkaline electrolyzer unit with bipolar electrode geometry.

The electrodes are made of electrocatalytic materials to ensure low overvoltages by facilitating rapid electrode-electrolyte charge transfer, and nucleation of the gas bubbles at the electrode surface as well as their self-detachment from the electrode surface at the operating cell voltage. To reduce the overvoltages the electrode should provide an interface between catalyst and the electrolyte of large surface area. Hence various electrode geometries have been used, including finned bodies, screens, perforated plates and flat

plates with electrochemically roughened surfaces [7]. The elements from group 8 (Fe, Ru, Os), 9 (Co, Rh, Ir) and 10 (Ni, Pd, Pt) and their alloys are conventionally used as electrode materials [31]. Noble metals like platinum and iridium have high catalytic activity with high corrosion resistance, however these materials are expensive and their use is limited to electrolysis using acidic media. Nickel, cobalt and iron (stainless steel) have low overpotentials in aqueous caustic soda or potash solutions and hence are used widely as cathodes for alkaline electrolysis [27,32-37]. Ni has high corrosion stability and hence both Ni electrodes and Ni coated steel electrode supports are common in alkaline electrolyzers, especially in those using elevated temperatures (above 80°C) and high concentration electrolytes [14]. Raney nickel is a porous material with high catalytic activity that shows low hydrogen overpotentials in alkaline solutions [7,38]. Advanced electroyzers prefer Raney nickel as the cathode material and perovskite oxides like $LaCoO_3$ and $LaNiO_3$ as anode materials [39].

Porous diaphragm-like separators are used to divide the anode and cathode regions to prevent mixing of the evolved hydrogen and oxygen gases while allowing for passage of the electrolyte solution. The pores of a separator must remain full of liquid so that gas cannot penetrate them, as well as allow passage of current without an appreciable resistance. Use of a separator allows adjacent placement of the electrodes thus reducing the Ohmic overpotential. A separator has pore sizes smaller than the diameter of the smallest gas bubble, for hydrogen this is around 10 μm, and to keep the electrical resistance low a porosity greater than 50%. Commonly used separator materials, which must be corrosion resistant and structurally stable, are asbestos [$Mg_3Si_2O_5$ $(OH)_4$], woven cloth, polymer materials like polytetrafluoroethylene (PTFE), oxide ceramic materials like NiO, and cermets like Ni-$BaTiO_3$ [21,30,40].

Water electrolyzer units typically consist of several cells or electrodes arranged in two basic configurations, tank type operated in unipolar configuration, or filter press type operated in bipolar configuration. The most common configuration, see **Fig. 2.1**, is the unipolar tank type where each electrode has only one polarity and all the electrodes of the same polarity are connected in parallel. The anodes and cathodes are alternately connected, with the

electrodes and separators kept immersed within an electrolyte containing tank. The unipolar tank cells require relatively simple construction, few parts, low cost, and are easy to maintain. However, they are also bulky and cannot be operated at high temperatures or pressures; the unipolar tank type cells normally operate at temperatures between 60°C and 90°C (higher temperatures result in rapid electrolyte evaporation) and near ambient pressure [30]. The relatively long current paths manifest in the leads and electrodes result in unwanted energy losses.

In bipolar filter press type configuration, see **Fig. 2.2**, the cells are connected in series with each cell consisting of a separator diaphragm pressed on either side by electrodes. An electrically conducting solid separator plate joins the electrodes in adjacent cells and serves as the partition between the hydrogen cavity of one cell and the oxygen cavity of the other. The electrode at one side of the separator plate acts as a cathode of one cell, whereas that on the other side acts as the anode of the adjacent cell. Advanced electrolyzers have a zero-gap geometry [20] with the anode and cathode directly formed on opposite sides of a porous diaphragm. The bipolar filter-type electrolyzers are relatively compact, and in comparison to tank type cells capable of operating at higher temperatures and pressures with lower Ohmic losses. The bipolar filter type cells can operate at temperatures as high as 150°C and pressures up to about 30 bar [23]. Consequently in comparison to tank type cells, filter-type electrolyzers can be operated at lower cell voltages with higher current densities. However, they need precise construction and they are more expensive and difficult to maintain.

Alkaline electrolyzers are used all over the world for electrolytic hydrogen production, delivering hydrogen with a nominal purity of 99.8%. Conventional cells operate at voltages 1.8-2.2 V with current densities below 0.4 A/cm^2; advanced electrolyzers operate at relatively lower voltages (as low as 1.6 V) and higher current densities (up to about 2 A/cm^2) [21,30]. Conventional tank-type electrolyzers have efficiencies in the range of 60-80%, while modern zero-gap electrolyzers can be up to 90% efficient. Hydrogen production rates in normal alkaline electrolyzers are between 0.01 and 10 m^3/h, whereas some large-scale units can reach 10 to 100 m^3/h. However, electrolyzers

suitable for large-scale hydrogen production necessarily have large-scale electrical power requirements, and there are environmental concerns related to the chemicals used in the electrolytes. Within the global energy context and the need to reduce CO_2 emissions, the most logical approach for hydrogen generation by water electrolysis appears to be the adjacent coupling of either windmills or photovoltaic grids (see Chapter 8) to the electrolyzer.

Solid Polymer Electrolyzers

The development of solid polymer electrolyte (SPE) water electrolyzers is coupled to the invention of proton exchange membrane (PEM) fuel cells [9,41,42]. In the mid 1950s researchers at the General Electric Corporation (GE) developed fuel cells using a sulfonated polystyrene electrolyte [41,42]. In 1966 fuel cells employing a much superior membrane, DuPont's Nafion, were developed and used for NASA space projects. In 1973 GE developed SPE water electrolyzers using proton exchange membrane technology that were initially used for oxygen generation in nuclear submarines [41]. SPE water electrolyzers have now become an industrially viable, well-accepted technology. These electrolyzers are compact and ecologically clean; in comparison to alkaline electrolyzers, SPE electrolyzers are able to operate at lower cell voltages, higher current densities, as well as higher pressures and temperatures. SPE electrolyzer efficiencies can reach near 100%, with normal device operation the 80-90% range [30,43,44]. An additional major advantage of SPE technology is that it can generate very high purity (>99.999%) hydrogen.

SPE electrolyzers, see **Fig. 2.3**, have a device configuration similar to that of zero-gap bipolar filter press type alkaline electrolyzers, see **Fig. 2.2**, but a proton conducting perfluorinated polymer membrane like Nafion (also known as perfluorosulfonic acid) having side chains terminated in sulphonate ion exchange groups, serves simultaneously as electrolyte and the separator [43]. Highly pure water circulated through the cell is split into hydrogen and oxygen with the help of electrocatalysts on the membrane surface. The membrane is normally a 150 – 300 μm thick sheet that is impermeable to water and product gases. It

possesses poor electronic conductivity but high proton conductivity when saturated with water. The sulfonic acid groups ($-SO_3H$) incorporated in the membrane become hydrated when exposed to water and then dissociate ($-SO^-_{3aq} + H^+_{aq}$) facilitating proton conduction [45]. On the anode, when in contact with water, hydroxy bonds are formed at the active surface sites, X, on the membrane with release of protons [46].

$$X+H_2O \rightarrow X\text{-}OH_{ads} + H^+ + e^- \quad (2.2.18)$$

The hydroxy bonds then break releasing more protons.

$$X\text{-}OH_{ads} \rightarrow X\text{-}O + H^+ + e^- \quad (2.2.19)$$

The protons, or more correctly hydrated protons ($H^+.nH_2O$), migrate through the membrane towards the cathode by hopping from one fixed sulfonic group to another; at the cathode they collect electrons and form hydrogen gas. The X-O bonds at the anode side then break and release oxygen gas, leaving the active sites free for another adsorption-desorption process. In addition to Nafion, materials like polyetheretherketone, polytetrafluoroethylene (PTFE), polyethylene, polybenzimidazole, polyimide, polyphosphazene and methyl methacrylate are also used to fabricate membranes for electrolysis after appropriate chemical modifications [33,47,48]. Methyl methacrylate monomer is an OH^- conductor instead of a proton conductor and hence the use of noble metal catalysts can be avoided.

The structure of a SPE cell is shown in **Fig. 2.3**. The basic unit of a SPE electrolyzer is an electrode membrane electrode (EME) structure that consists of the polymer membrane coated on either side with layers (typically several microns thick) of suitable catalyst materials acting as electrodes [43,49,50], with an electrolyzer module consisting of several such cells connected in series. The polymer membrane is highly acidic and hence acid resistant materials must be used in the structure fabrication; noble metals like Pt, Ir, Rh, Ru or their oxides or alloys are generally used as electrode materials. Generally Pt and other noble metal alloys are used as cathodes, and Ir, IrO_2, Rh, Pt, Rh-Pt, Pt-Ru etc. are used as anodes [43,46]. The EME is pressed from either side by porous, gas permeable plates that provide support to the EME and ensure

homogeneous current distribution across the membrane surface. These porous plates provide exit paths for the gas generated at the electrodes. Titanium and carbon are the commonly used materials at the anode side whereas carbon is the preferred material at the cathode side. The bipolar plates are in direct physical contact (see **Fig. 2.3**) with the porous structures that separate adjacent cells while allowing the current to pass from one cell to the next. The cavity between the bipolar plate and current collector allows the distribution of feed water and the collection of product gases. The plate material must have high electronic conductivity, negligible permeability to product gases, and high corrosion resistance. Graphite is generally used for making the bipolar plates.

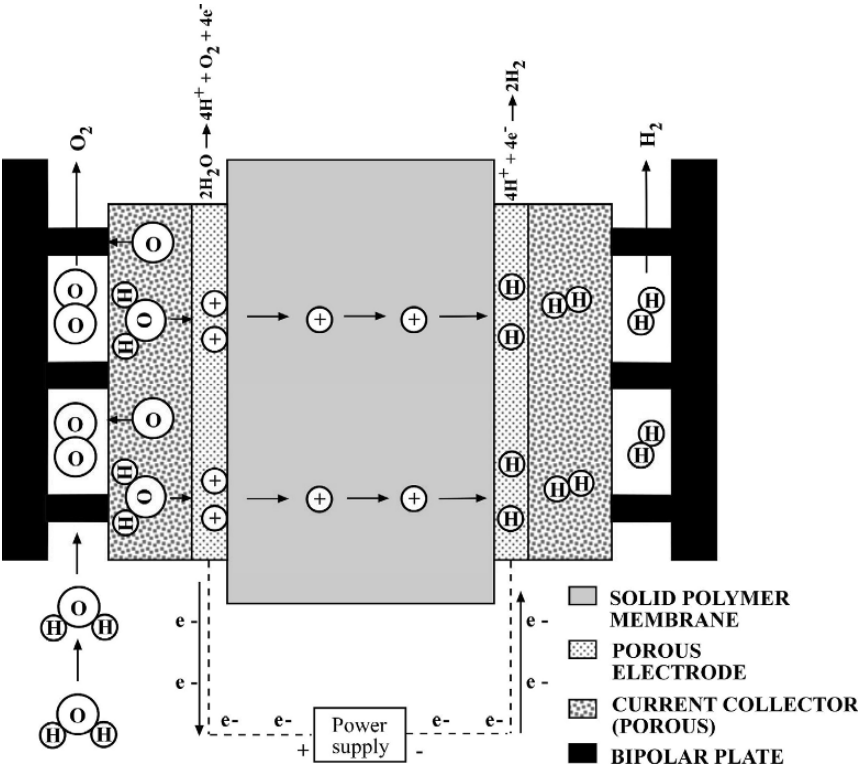

Fig. 2.3: A solid polymer electrolyte (SPE) cell configuration.

In comparison to alkaline electrolyzers, SPE electrolyzers are more efficient, reliable, and safer. Since SPE electrolyzers use solid electrolyte, there is no risk of corrosive chemical leaks nor issues of unwanted gas cross-over. As the cells in SPE electrolyzers are connected in series high voltage dc supplies can be used which are less expensive compared to the low voltage high current dc supplies. Currently these cells generally operate at temperatures of 80-150°C and pressures of about 30 bar [30], with high pressure (≈ 135 bar) SPE electrolyzers being developed. Cell voltages range from 1.4 V to 2 V, with current densities up to about 2 A/cm^2. These cells can intrinsically adjust to variations in electrical power hence are well suited for operation using power from inherently intermittent solar cells or wind mills. However, SPE electrolyzers are comparatively expensive due to the high cost of the polymer membranes and noble metal electrodes, as well as requiring very high purity water. Other design nuances are that precise control of the differential pressure across the anodic and cathodic compartments is necessary for membrane stability. In thin membranes hydrogen diffusion to the anode can adversely affect device efficiency [23].

Solid Oxide Electrolyzers

Solid oxide electrolyte (SOE) cells were first developed in the early 1970s [5]. These cells operate at very high temperatures, near 1000°C, exploiting the useful effects of high temperatures on the kinetic and thermodynamic parameters controlling electrolytic water splitting to generate hydrogen from steam. The total energy demand for water splitting ΔH is lower in the vapor phase (241.8 kJ/mol) than in the liquid phase (285.83 kJ/mol) [10,12]. The thermoneutral voltage is around 1.287 V at 800°C [51]. As discussed at the beginning of this section, high temperatures lower the thermodynamic reversible potential for water splitting as well as the activation overpotentials. Thus the electrical energy requirements are much lower for water electrolysis in vapor phase at high temperatures. The extra energy needed to drive the reaction is supplied as heat, which is more efficient to obtain and hence cheaper than electricity. **Figure 2.4** shows the demand of electrical and heat energies with electrolysis temperature. It can be seen from **Fig. 2.4** that the ratio of ΔG

(electrical energy demand) to ΔH (total energy) is about 93% at 100°C and about 70% at 1000°C, which shows that in high temperature electrolysis about 30% of the energy involved can be supplied as heat [52]. The heat requirements of the cell can be met either internally through Ohmic heating or externally using a heat source depending upon whether the operation is allothermal or autothermal. The reduced electrical energy requirements enables the SOE cells to operate at lower voltages (about 0.95 to 1.33 V) than those required for other types of electrolyzers [30].

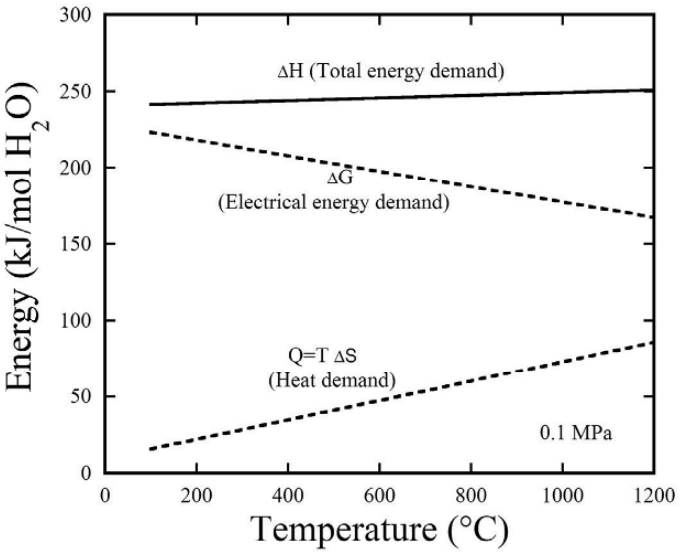

Fig. 2.4: Requirement of electrical and heat energies for steam electrolysis.

SOE cells utilize solid ceramic electrolytes (e.g. yttria stabilized zirconia) that are good oxygen ion (O^{2-}) conductors at very high temperatures in the range of 1000°C [8]. The operating temperature is decided by the ionic conductivity of the electrolyte. The feed gas, steam mixed with hydrogen, is passed through the cathode compartment. At the cathode side, the reaction is

$$2H_2O+4e^- \rightarrow 2H_2+2O^{2-} \qquad (2.2.20)$$

As the electrolyte is impermeable to hydrogen gas, the O^{2-} ions migrate through the electrolyte towards the anode under the action of the electric field, where they gain electrons and form oxygen gas.

$$2O^{2-} \rightarrow O_2+4e^- \qquad (2.2.21)$$

The electrolyte is impermeable to water vapor and product gases, thus it effectively separates hydrogen and oxygen.

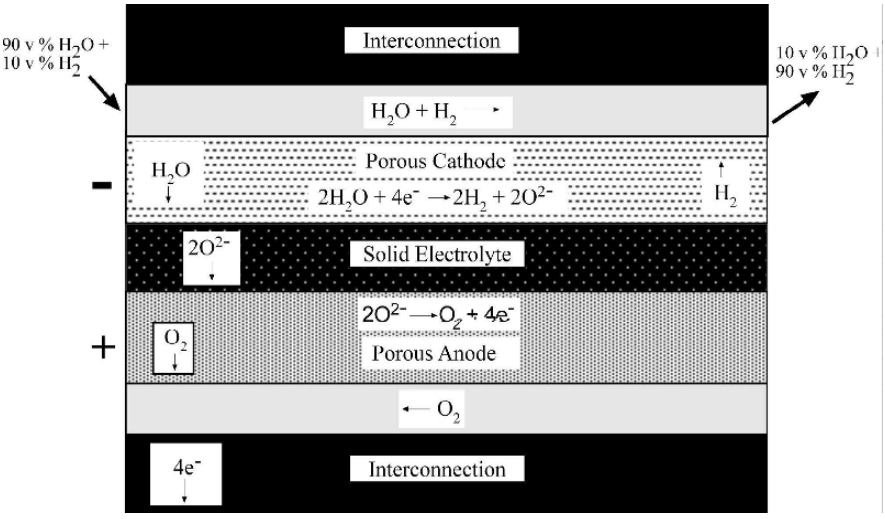

Fig. 2.5: A solid oxide electrolyte (SOE) electrolyzer configuration (planar geometry).

SOE cells are fabricated in planar, see **Fig. 2.5**, as well as tubular geometries [51-55], with the voltage and current losses minimized in the planar geometry. In both planar and tubular cases the electrolyte is pressed between porous electrodes. The cells are attached in series using interconnecting elements that serve as electrical conductors as well as current distributors. The cells with planer geometries are simply stacked to form the electrolyzer unit. In the tubular geometry each cell is fabricated in the shape of a short circular tube, which are then connected along their lengths forming a long tube; the electrolyzer module consists of a stack of several such tubes. The feed gas is passed through the inner surface of the tube and oxygen is evolved through the outer surface. Although a number

of solid oxide electrolytes have been tested, yttria stabilized zirconia is the favorite electrolyte material of today [56]. Cermets such as Ni-ZrO_2 and Pt-ZrO_2 are commonly used as cathode materials, and conducting perovskites like $LaNiO_3$, $LaMnO_3$, and $LaCoO_3$ used as anodes [57]. Materials like Ferritic steel and doped $LaCrO_3$ are used to make the interconnections, and $CaZrO_3$ used for insulation of the assembly.

We note that SOE cell technology is still in the developmental stage. Severe materials problems related to the high temperature operation, typically 700-1000°C, need to be solved. Low life times of the materials used for cell construction, intermixing of adjacent phases and engineering problems related to thermal cycling and gas sealing are some of the factors that prevent the technology from successful commercialization [8]. However, this technology has some unique advantages that make it attractive in comparison to other technologies [58]. Compared to other types of electrolyzers the power consumption is less; in comparison to advanced alkaline electrolyzers [59] SOE cells require at least 10% less energy. The efficiency of high temperature electrolysis can essentially be 100% [30]. Furthermore SOE electrolyzers are relatively eco-friendly, not requiring any corrosive electrolytes for operation [58].

2.3 Hydrogen Production by Thermochemical Water-Splitting

Thermochemical processes utilize thermal energy, either directly or through different chemical reactions, to carry out water splitting for hydrogen generation. The net reaction is

$$H_2O + \text{thermal energy} \rightarrow H_2 + \tfrac{1}{2} O_2 \qquad (2.3.1)$$

A portion of the supplied thermal energy is expelled with the products. The overall water splitting process, see **Fig. 2.6**, in general requires both heat and work input. In **Fig. 2.6** q_r represents the heat energy supplied at high temperature T_r, q_0 represents the heat rejected at lower temperature T_0, and W_i is the useful work input, if any, for the process. The enclosed region contains only water, or water and materials involved in different

reactions. Water is supplied into the enclosed region where it is split using thermal energy, releasing hydrogen and oxygen as the by-products.

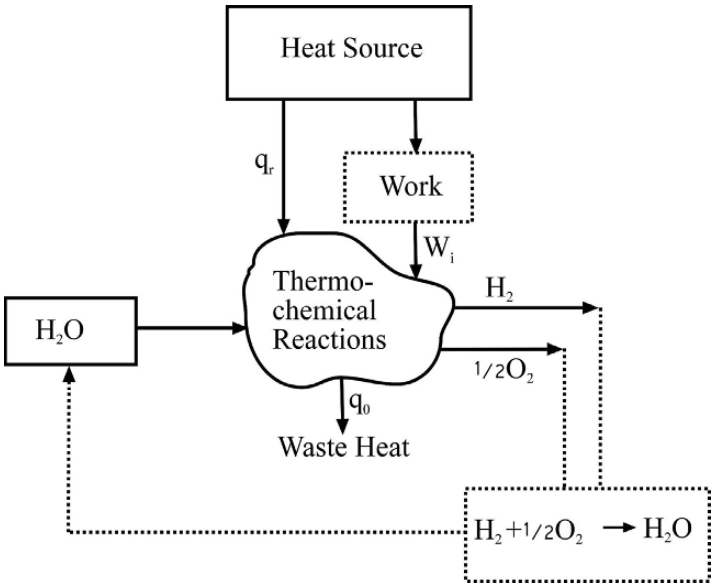

Fig. 2.6: General representation of the thermochemical water splitting process

As the water splitting process is cyclic (reversible behavior shown by dotted lines in **Fig. 2.6**) it has limitations imposed by second law of thermodynamics [60]. Hence the operating temperatures T_r and T_0 are crucial in determining the thermal efficiency of the process. In a water splitting process using both heat and work inputs, the thermal efficiency in general is defined as [60,61]

$$\varepsilon = \Delta H_0/(\sum_r q_r + \sum_i W_i/ \xi_i) \qquad (2.3.2)$$

Where q_r represents the heat input from different sources, W_i the useful work input and ξ_i denoting the heat to useful work conversion efficiency associated with it. Depending upon the process, work input W_i may be required for different process steps like driving the reaction, reaction-product separation, and mass transfer. ΔH_0 is the

enthalpy change involved in water splitting; generally the higher heating value (HHV) of hydrogen is assigned to ΔH_0 in equation (2.3.2) [62].

Equation (2.3.2) shows that a reduction in work input W_i is necessary if, realistically, high operating efficiencies are to be obtained. If the work input is zero, i.e. if only thermal energy is supplied, using the first and second laws of thermodynamics it can be shown that [2,4,60,61]

$$\varepsilon \leq (\Delta H_0/\Delta G_0)\,[(T_r - T_0)/T_r] \qquad (2.3.3)$$

Here $T_r - T_0/\ T_r$ is the Carnot efficiency of a heat engine working between T_r and T_0 [60]. This relation gives the maximum attainable thermal (heat to heat conversion) efficiency of an ideal water splitting process. The efficiency of an ideal process reaches over 80% when T_r and T_0 are, respectively, 1200 K and 393 K [3]. This indicates that high efficiencies are possible if water splitting can be done at high temperatures. It should be noted that a parameter that is important for assessing the commercial viability of a thermochemical process is the exergy (useful work) efficiency [63,64]. The exergy efficiency is defined as the ratio of the Gibbs free energy of the water formation reaction to the total energy necessary to split water using a thermochemical cycle. Exergy analysis gives the information about the requirements and losses in each process component. However, in the following discussion 'efficiency' implies thermal efficiency.

Emil Collett, in 1924, hypothesized a two-step water splitting process involving mercury and mercury oxide that, while a remarkable idea, was later proved infeasible [4,65]. In 1960s the interest in utilizing nuclear waste heat for useful purposes like hydrogen production initiated research in practical thermochemical water splitting [1], as pioneered by Funk and Reinstrom [60]. The 1973 oil embargo motivated significant research efforts in thermochemical hydrogen production [1-4] that were subsequently abandoned due to lack of financial support when the immediate energy crisis passed.

Historically, the initial objective behind the use of thermochemical processes for water splitting was to produce

hydrogen directly from the heat released by nuclear waste, rather than through a waste heat- electricity- electrolysis route in which the overall efficiency of hydrogen production is the product of the electrical energy production efficiency and the electricity-to-hydrogen conversion efficiency. The low thermal to electrical energy (useful work) conversion efficiency in the waste heat-electricity- electrolysis route reduces the overall efficiency of hydrogen production. For example, the overall efficiency of hydrogen production from an advanced electrolyzer working at an efficiency of 90% using the electricity produced from a nuclear reactor at an efficiency of 40% (present day feasible value) is 36%. However, the overall thermal to hydrogen conversion efficiency in the thermochemical water splitting process can be 50% or above [66,67]. A 50% efficient process can produce 10 tons of hydrogen a day from a 30 MW thermal energy source.

The maximum temperature of a high temperature nuclear reactor, as determined by safety considerations, is 1573 K [68]. Selection of a suitable reactor type for thermochemical hydrogen production depends upon whether the coolant used in the reactor can effectively transfer the heat to a thermochemical process. Studies show that high temperature gas cooled reactors (HTGR), molten-salt-cooled reactors (MSR), and heavy metal cooled reactors (HMR) are the most suitable candidates for thermochemical hydrogen production technology [69]. Of these helium-based HTGR are appropriate for use in processes operating in the range of 1100-1300 K. The environmental as well as safety concerns regarding the use of nuclear reactors are, of course, applicable to the nuclear-thermochemical technology.

Thermochemical water splitting, making use of concentrated solar radiation for supplying the necessary thermal energy to drive the reactions, is a promising technology. Very importantly this solar energy based approach is renewable, while very high temperatures can be achieved that far exceed those obtainable with nuclear reactors. This high temperature operation offers higher ideal thermal efficiency according to equation (2.3.3). The concentrators collect the solar radiation and focus it into the chamber where reactions take place. Depending upon the geometry of the concentrators, parabolic trough, tower, dish etc., different concentration ratios and hence

temperatures can be achieved [70-72]. Temperatures up to about 3000 K can be obtained using concentration ratios in excess of 10000 suns [70]. Hence the technology is particularly useful for thermochemical cycles that require very high temperatures. However, solar concentrators require space, and the installations are in practice limited to the desert or sun-belt regions of the world (of which there are many) where there are minimum diurnal and seasonal variations. Different options have been considered to avoid shut down of thermochemical plants during cloudy days. One option is to store solar energy in a thermal storage system during sunshine hours while simultaneously using the solar energy directly for running the thermochemical plant [73].

Different strategies have evolved for thermochemical hydrogen production to effectively utilize the potentials of, in particular, nuclear and solar thermal energy sources. These strategies, which we discuss below, can be categorized depending upon the number of process steps involved and whether electrolysis is employed in a reaction.

One-step Thermochemical Process

In a process called direct thermolysis, at a high enough temperature thermal energy is sufficient to split water into hydrogen and oxygen. Only one reaction is involved in this process, that of equation (2.3.1). In **Fig. 2.6**, if the input water and output gas mixture are at the same temperature T_0, the minimum work input required to effect water splitting at temperature T_r can be written [60]

$$W_r = \Delta G = \Delta G_0 - \Delta S\,(T_r - T_0) \qquad (2.3.4)$$

where ΔG and ΔG_0 are, respectively, the free energy changes when the reaction is carried out at T_r and T_0. ΔS does not increase significantly with temperature [3]. Thus the useful work requirement reduces on increasing the reaction temperature T_r. At a pressure of 1 bar ΔG becomes zero at about 4300 K [1,3,70]; at this operating point 100% of the water molecules are split. Only partial dissociation of the water molecules is achieved at lower temperatures. At 2000 K and 1 bar pressure about 1% of water is

split; this increases to about 9% at 2500 K, and 36% at about 3000 K [3]. The fraction dissociated at a particular temperature increases with a reduction in pressure. At 2500 K and 0.05 bar about 25% of the water is dissociated.

When water splitting occurs in the temperature range 2000 to 3000 K, 1 bar pressure, only H_2O, OH, H, O, H_2 and O_2 exist in significant concentrations (and in different molar ratios); the possibility of the presence of species such as HO_2, O_3 and H_2O_2 can be neglected [74-77]. To achieve any reasonable yield of H_2 using direct thermolysis the temperature should be around 3000 K or above. For example, at 2500 K and 1 bar, direct thermal water splitting can yield about 4% molecular hydrogen (H_2 species) [3]. Nevertheless, due to materials limitations at this high temperature the preferred operating temperature regime of today is 2000- 2500 K [74]. As the water splitting reaction is reversible, and hydrogen yield is low in the 2000- 2500 K temperature regime, hydrogen and oxygen should be separated in a timely manner before they can recombine to form water.

As noted, separation of the evolved hydrogen and oxygen is an important step in any thermochemical water splitting cycle. Rapid separation of the gases is required not only to avoid efficiency loss due to hydrogen-oxygen recombination, but also to avoid hydrogen and oxygen forming an explosive mixture. Among the different methods available for product separation, methods such as quenching and high temperature separation are appropriate for a one step process [74-76,78]. In the quenching method, the hot product gas is rapidly cooled to 450 K using low-temperature steam or inert gas [74], then further cooled to remove water vapor through condensation. The mixture of dry oxygen and hydrogen are then separated using non-porous solid membranes like palladium or palladium-silver alloys. Quenching is not an energy efficient process as it is not possible to retrieve the energy contained in the un-split water cooled along with product gas mixture.

In high temperature separation, hydrogen is separated from the hot product gas at the reaction temperature using porous membranes made of materials such as zirconia. The porous membranes separate the gases through, in general, either mass diffusion or molecular effusion [3,74,79]. In mass diffusion, the

gases are separated by the difference in the diffusion coefficients of the component gases with respect to an auxiliary gas like water vapor [3]. In molecular effusion, hydrogen is separated from the reacting gas mixture by effusing through the porous ceramic membrane in the Knudsen flow regime. For this process to occur the pore size is kept less than the mean free path of hydrogen at the separation temperature and pressure. This process is efficient and hence recommended for one-step process. The hot unused steam rejected after the selective effusion of hydrogen can be further dissociated using high temperature electrolysis. Compared to other separation processes this hybrid process is considered more efficient and economical [74]. Instead of porous membranes, solid oxygen ion conductors like zirconia can also be used to remove oxygen from the hot gas by applying an electrical bias across the membrane.

The high temperatures needed for the one-step process can only be supplied using solar energy concentrators. The reaction is usually conducted in a cavity where the solar radiation is focused through a quartz window using dish type mirrors with large collection areas. Materials used for cavity construction need to be able to withstand extremely high temperatures and large temperature fluctuations; as of today graphite (in inert ambient) and zirconia are the preferred materials [75]. Immediately after formation hydrogen is separated from the mixture; the hot gases are then passed through heat exchangers for cooling and then compressed for storage and use. The theoretical efficiency of the process is about 64% at 2500 K and 1 bar [71]. Although the water splitting yield is higher at pressures below 1 bar the overall efficiency is considerably less due to the high work input needed to compress the hydrogen [80].

Direct thermal water splitting is an environmentally benign technology that, once the system is built, requires only solar energy and water. The process efficiency is high due to the high temperatures involved. However the high operating temperatures, i.e. 2000 K to 3000 K, pose severe challenges to the materials used for construction of reaction chamber, separators and heat exchangers. At the reaction temperature gas separation, and collection of the various hydrogen species, is difficult. Furthermore re-radiation from the reactor at these extreme temperatures lowers the absorption efficiency [81]. In the 2000 to 3000 K temperature

range a significant amount of water entering the reaction chamber is heated without undergoing dissociation [3,81,82]. For achieving reasonably high practical efficiencies, methods to effectively recover high temperature heat from this unutilized steam need to be implemented. Hence at present the direct thermal splitting of water is not considered an economically viable technology that can be used for commercial hydrogen production.

Two-step Thermochemical Processes

If water splitting is performed through more than one step, let us say *j* reactions with the reactions occurring at different temperatures, then the minimum useful work requirement given in equation (2.3.4) can be written as [2,60,61]:

$$W_r = \Delta G = \Delta G_0 - \sum^{i=j}_{j=1} \Delta S_i \, (T_{r(i)} - T_0) \qquad (2.3.5)$$

Thus, by selecting reaction steps with appropriate ΔS and T_r values it is theoretically possible to reduce the work input to zero while minimizing the T_r of each reaction. That is to say, when more than one reaction step is involved water splitting can be done using thermal energy at much lower temperatures than that required for a single step process. The simplest example of this is, of course, a two-step process. Two-step processes involving metal oxide cycles are largely considered the most promising. The process, in general, consists of the following steps

$$\text{Metal oxide} \rightarrow \text{Reduced metal oxide} + O_2 \text{ (endothermic)} \qquad (2.3.6)$$
$$\text{Reduced metal oxide} + 2H_2O \rightarrow \text{metal oxide} + 2H_2 \qquad (2.3.7)$$

In the first step, a high valence metal oxide is reduced to a low valence metal oxide or a low valence metal oxide is reduced to the corresponding metal by the high temperature heat energy, releasing oxygen. The metal or oxygen deficient metal oxide then reacts with water at a lower temperature releasing hydrogen and regaining stoichiometry. The net reaction is the splitting of water into hydrogen and oxygen. The temperature range required for the first reaction is about 1700-3000 K. Hence, for practical applications the option is limited to the use of heat from concentrated solar radiation.

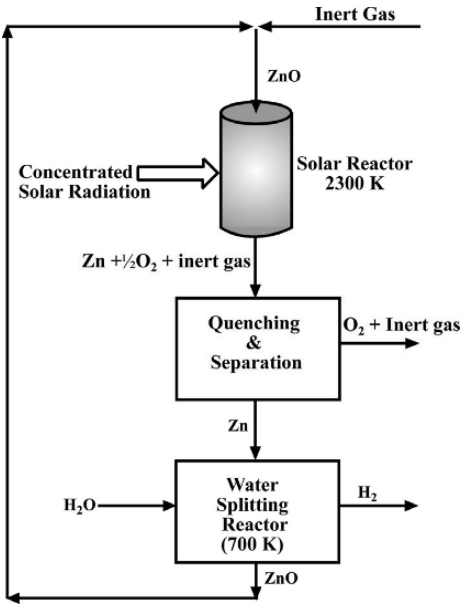

Fig. 2.7: Process flow schematic of a two-step Zn/ZnO cycle.

In 1977, Nakamura proposed a two-step cycle involving the Fe_3O_4/FeO redox pair [80]. Since then many metal oxides systems including Co_3O_4 /CoO, Mn_2O_3/ MnO, TiO_2/TiO_x, ZnO/Zn and different oxide ferrite systems like $ZnFe_2O_4/Zn/Fe_3O_4$ have been proposed by different groups [83-89]. Of these materials the ZnO/Zn pair is considered the most promising [70,88,90,91]. The ZnO/Zn cycle, see **Fig. 2.7**, consists of the following reaction steps

$$ZnO \rightarrow Zn + 0.5O_2 \qquad \text{(at 2300 K)}$$
$$Zn + H_2O \rightarrow ZnO + H_2 \qquad \text{(at 700 K)}$$

Zinc oxide in solid or fine particle form is kept in a reactor cavity that is subjected to irradiation from solar concentrators [92]. The dissociation products are zinc (vapor) and oxygen; for this first reaction $\Delta G=0$ at about 2235K [91]. The reactor is made of materials like inconel steel, zirconia, silicon carbide or graphite [68,89,92]. The graphite is used in special designs to avoid direct contact with chemical species [68]. The dissociation products are then cooled rapidly to separate zinc and oxygen, transporting the

products using an inert carrier gas to a low temperature zone. In this zone oxygen escapes, and zinc exists in fine liquid or solid particulate form [90] that is subjected to hydrolysis by passing steam. Zinc reacts with water and forms zinc oxide while releasing hydrogen [68,90,91,93], and the remaining zinc oxide is now available to begin the next cycle. A Zn to ZnO conversion rate of 83% by hydroloysis was reported by Wegner and co-workers [90]. The cycle needs only water as a feed material, and produces hydrogen and oxygen as products. The theoretical thermal efficiency of this cycle is 53% [94], whereas the exergy efficiencies at solar concentration ratios of 5000 and 10000 suns without considering any heat recovery are 29% and 36% respectively [91].

Compared to a single step process, two-step processes need lower temperatures yet provide a higher hydrogen yield (ratio of amount of hydrogen actually produced to maximum amount of hydrogen that can be produced). The product gas separation is relatively easy in a two-step process as oxygen and hydrogen are produced in two separate stages. No corrosive chemical is involved in the process. For many two-step cycles involving a metal oxide, the high temperature reaction is carried out around 2000K, which can be achieved using solar concentration ratios between 1000 and 5000 suns. This simplifies the solar concentrator design and implementation. However, this technology is still in its infancy due to a number of practical problems. For example, high temperature re-radiation loss is a major concern, which needs to be minimized using appropriate materials and designs for the reactor windows [91]. Also, after dissociation of the oxide there is a tendency for metal/reduced metal oxide and oxygen to recombine when the metal/reduced metal oxide cools as it proceeds towards the lower temperature zone [68]; rapid cooling is required to prevent this. High temperature sintering of the metal oxide particles is another problem, which effectively deactivates the metal oxide for subsequent cyclic reactions. Solid metal deposits on the reactor walls also need to be removed periodically. Finally the temperature regime used in a two-step metal oxide process is still not low enough to enable large-scale hydrogen production. As in the case of a one-step process, finding durable construction materials for different components of the reaction chamber remains an un-solved

challenge. As of today, the overall practical efficiency of this process is not high enough to compete with electrolysis.

Multi-step Thermochemical Processes

Multi-step cycles are designed in accordance with equation (2.3.5) in such a way that the maximum temperature required for any reaction in the cycle is limited to the temperature that can be supplied from a nuclear reactor [2,4,95], approximately 1500K. Furthermore all the chemicals involved in the reaction are confined to the enclosed region in **Figure 2.6** within a closed cycle, the operation of which is essential to avoid heat and material losses. With recycling of the chemicals only water is consumed, generating hydrogen and oxygen.

The suitability of a cycle for hydrogen production depends upon the overall thermal efficiency and operational feasibility. A highly endothermic reaction step is required in a cycle to achieve effective heat-to-chemical energy conversion. For efficient mass and momentum transfer a fluid based system is preferred [96] and, ultimately, for large-scale hydrogen production other factors such as environmental effects and cost effectiveness must also be considered.

The first multi-step process having a theoretical efficiency above 50% was proposed by Marchetti and Beni in 1970 [2]. This process became the *Mark-1* process of the European Commission's Joint Research Center (JRC), Ispra, Italy. A large number of cycles with reasonably high efficiencies were designed after this; Abanades and co-workers have recently made a compilation of the available thermochemical cycles that yielded about 280 cycles [67]. A large number of cycles are listed in references [2,4,67,95,97]. However only a few of these processes have exhibited potential for high overall efficiencies and technical feasibility. We discuss a few cycles that are presently under study and promising for practical implementation.

Sulfur-iodine Cycle

This cycle was developed by General Atomics Corporation in the mid 1970s [88,99]; the Japanese atomic energy research institute (JAERI) has also been actively involved in developing their version

of this cycle [100-103]. The reaction steps involved in this cycle are given below.

$$H_2SO_4 \rightarrow SO_2 + H_2O + \tfrac{1}{2}\, O_2 \qquad \text{(at 1123 K)}$$
$$I_2 + SO_2 + 2H_2O \rightarrow 2HI + H_2SO_4 \qquad \text{(at 393 K)}$$
$$2HI \rightarrow I_2 + H_2 \qquad \text{(at 723 K)}$$

A typical sulfur-iodine (S-I) process flow diagram is given in **Fig. 2.8**. The reactions are carried out in three different compartments [102-104]. The sulfuric acid decomposition is a high temperature endothermic process. The second step is the Bunsen reaction (exothermic) where sulfuric and hydrioidic acids are produced from iodine and sulfur dioxide in aqueous solution. In a critical step the sulfuric acid and hydriodic acids are separated in liquid phase, then purified and concentrated. For facilitating effective separation an excess of molten iodine is used in this reaction to form two separate phases, a *light* phase of sulfuric acid and *heavy* phase containing hydrogen iodide and iodine [99,103]. In an endothermic process the hydriodic acid is decomposed at a lower temperature to hydrogen and iodine. The net reaction is splitting of water into hydrogen and oxygen.

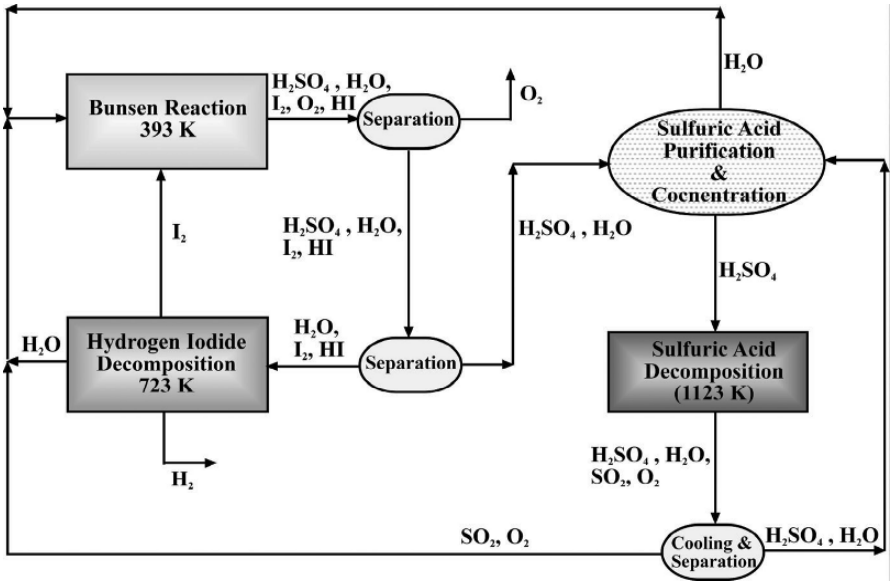

Fig. 2.8: Process flow schematics of a sulfur-iodine cycle.

The S-I cycle consists of reactions all taking place at moderate temperatures that can be achieved using nuclear waste heat, or concentrated solar rays sufficient to achieve temperatures comparable to its nuclear counterpart. According to the claims made by different groups regarding the efficiency of the S-I cycle, the values of efficiency lie in the range 42 to 56.8% showing this to be one of the most efficient cycles [68,100,105]. All reactions involved in the S-I cycle are fluid based, and there are no effluents. However there remain technical challenges. The reactions involving decompositions of sulfuric acid and hydriodic acid create an aggressive chemical environment and hence chemically stable materials must be used in construction of the process chamber. After the Bunsen reaction, a complete removal of the sulfuric acid from the hydriodic acid phase is necessary to avoid sulfur formation in the HI separation and HI decomposition steps. Further, complete recovery of hydrogen from HI and I_2 from the last reaction is difficult, limiting the process efficiency. In the sulfuric acid decomposition step SO_3 can be formed along with SO_2 that needs to be promptly separated. To eliminate problems associated with SO_3 an operating temperature above 1400K is necessary [104].

The UT-3 cycle

The UT-3 cycle was named after the University of Tokyo where the process was developed in late 1970s. As of today the UT-3 cycle is considered to have the greatest potential for commercialization. UT-3 cycle is a four-step process involving the reactions [73,106-110]

$$CaBr_2\ (s) + H_2O\ (g) \rightarrow CaO\ (s) + 2HBr\ (g) \quad \text{(at 1033 K)}$$
$$CaO\ (s) + Br_2\ (g) \rightarrow CaBr_2\ (s) + \tfrac{1}{2}\ O_2\ (g) \quad \text{(at 845 K)}$$
$$Fe_3O_4\ (s) + 8HBr\ (g) \rightarrow 3FeBr_2\ (s) + 4H_2O\ (g) + Br_2\ (g) \quad \text{(at 493 K)}$$
$$3FeBr_2\ (s) + 4H_2O\ (g) \rightarrow Fe_3O_4\ (s) + 6HBr\ (g) + H_2\ (g) \quad \text{(at 833 K)}$$

The first two reactions ensure the formation of hydrobromic acid releasing oxygen, and the other two ensure the reduction of water releasing hydrogen. The reaction takes place in four separate reactors in isothermal or adiabatic conditions. The reactors are paired; one pair contains calcium compounds (reaction 1 and 2) and

the other contains iron compounds (reactions 3 and 4). The complete cycle takes about an hour to complete. After each cycle the functions of the paired reactors are switched so that reactor 1 now carries CaO and reactor 2 contains $CaBr_2$ (similarly reactors 3 and 4), thus producing hydrogen and oxygen continuously without transferring solid products from one reactor to the other. The theoretical thermal efficiency of a UT-3 hydrogen production system is around 49%, and exergy efficiency is about 53% [73,107]. One limitation of the processes is that the solids used in the cycle, especially those working near their melting points, could suffer structural changes due to sintering effects leading to deterioration of process efficiency. Operational issues associated with alternately switching the reactors for exothermic and endothermic reactions have yet to be effectively addressed.

The Copper-Chlorine cycle

In comparison to the S-I and UT-3 cycles the Cu-Cl cycle is attractive due to the significantly lower reaction temperatures [69,111]. The cycle reactions consists of [66]:

$$2CuCl \rightarrow CuCl_2 + Cu \qquad (\text{at} < 373\ \text{K})$$
$$2CuCl_2 + H_2O \rightarrow CuO.\ CuCl_2 + 2HCl \qquad (\text{at } 573\text{-}648\ \text{K})$$
$$CuO.\ CuCl_2 \rightarrow 2CuCl + \tfrac{1}{2}\ O_2 \qquad (\text{at } 723\text{-}803\ \text{K})$$
$$Cu + HCl \rightarrow CuCl + \tfrac{1}{2}\ H_2 \qquad (\text{at } 698\text{-}723\ \text{K})$$

This cycle uses solid reactants. Small dendritic copper particles are used to carry out the last reaction to make the transformation of all the solid copper to CuCl, thereby maximizing hydrogen yield. The reported efficiency of this cycle is 49% [66]. This low temperature cycle is believed to eliminate many of the engineering and materials issues associated with the other two previously discussed cycles, however this cycle is also in the initial stages of development [111]. The temperature ranges are such that lower temperature nuclear reactors, e.g. sodium-cooled fast reactors, could be used with this cycle [69]. A hybrid version of this cycle is under investigation in Argonne National Laboratory [66,112].

In general, the efficiency of a multi-step process reduces with increasing number of reaction steps due to thermal losses, and difficulties involved in product separation from each reaction. However if thermochemical technology is to be implemented to put the hydrogen in a hydrogen economy then multi-step processes appear as the favorite candidates for large-scale hydrogen production. Compared to one-step and two-step processes, in practice these cycles offer much better efficiencies (> 50%) and are believed to have comparatively low capital and operating costs. Hydrogen and oxygen are produced in separate reactions hence costs associated with separation are avoided. While in multi-step processes there is greater potential for the presence of hazardous impurities in the hydrogen and oxygen product streams, which may necessitate purification facilities to meet health and environmental standards, still it appears that volume scale hydrogen can be realistically produced at a purity in excess of 99.99%.

Hybrid Thermochemical Processes

Hybrid thermochemical processes use both heat and work inputs, with at least one of the reactions driven by electricity. The electricity driven, electrochemical reaction is selected in such a way that the overall work input is much less than that required for water electrolysis. An advantage of this technology is the possibility to establish two-step processes that require much lower temperatures compared to the pure two-step thermochemical cycles and hence greater simplicity in the chemical processes. Several hybrid cycles were developed during the 1970s and 1980s [2,113,114]. A hybrid cycle initially studied at Los Alamos Scientific Laboratory and developed by Westinghouse Corporation in 1975, called the sulfuric acid hybrid cycle or the Westinghouse sulfur process (WSP) is considered promising and still under study [65,97,114-118]. This process is named the Mark 11 cycle by the European commission's Joint Research Center (JRC), Ispra, Italy [T24]. The reactions involved are:

$$H_2SO_4 \rightarrow SO_2 + H_2O + \tfrac{1}{2}\, O_2 \qquad \text{(at 1100 K)}$$

$$2H_2O + SO_2 \rightarrow H_2SO_4 + H_2 \qquad \text{(electrolytic; at 363 K)}$$

The reversible potential for the sulfur dioxide electrolysis is only 0.17 V, less than 10% that of water electrolysis (minimum of 1.23V at 298K and 1 bar) [65,69]. However corrosion problems in the electrolysis step are severe due to the presence of high concentration (about 50%) sulfuric acid. The overall thermal efficiency of the process, considering both thermal and electrical energy input derived from the same heat source, is estimated as 48.8% [116]. However, in terms of economics and process complexity the hybrid cycles face tough competition from advanced water electrolyzers.

2.4 Hydrogen Production By Water Biophotolysis

Biophotolysis is the process of splitting water into hydrogen and oxygen through a series of biological activities utilizing solar radiation. The overall process can be represented as

$$H_2O + \text{light energy} \xrightarrow{\text{(biological activity)}} H_2 + \tfrac{1}{2} O_2 \qquad (2.4.1)$$

Biophotolysis is an attractive method for generating hydrogen as it is both renewable and environmentally friendly. As the whole process involves only plants, sunlight and water, all the components in the process can be recycled producing no hazardous wastes. Carbon dioxide is recycled in this process and hence there is no net accumulation of this greenhouse gas. It is considered as a method for harvesting hydrogen directly, rather than obtaining hydrogen by planting, harvesting and processing of biomass. In principle, biophotolysis requires lower initial investments compared to other hydrogen generation processes.

Biophotolysis has its root in photosynthesis. Photoautotrophic plant species, both micro and macro, generate carbohydrates needed for metabolism using solar energy and water through the photosynthesis process. This process of converting solar energy to chemical energy utilizes water as an electron donor. It consists of a series of visible light induced redox reactions leading to the reduction of carbon dioxide received from the atmosphere and formation of carbohydrates. Photosynthesis involves light dependent

and light independent processes, with photosynthetic systems in plants and algae consisting of various complex components such as light-harvesting antennae, energy and electron-transfer systems, and redox centers.

The light dependent processes take place in the thylakoid membrane located in the chloroplast. The light harvesting takes place in two separate light absorbing membrane-integrated protein complexes each containing pigments tuned for light absorption in the visible region of the solar spectrum. These are denoted as Photosystem I and II (PS I and PS II) according to the chronological order in which these were discovered [119,120]. Each photosystem contains an array of light absorbing pigments called antenna pigments and a reaction center. The antenna consists of *chlorophyll a* and accessory pigments like *chlorophyll b, c* and *d*, *carotenes, xanthophylls* and *phycobiliproteins*. The presence and amount of the accessory pigments vary from species to species. The reaction center is a *chlorophyll a* protein complex consisting of an interacting pair of chlorophyll molecules. The reaction centers in PS I and PS II are denoted, respectively, as P_{700} and P_{680} according to the wavelength in the red region at which maximum light absorption occurs. P_{680} has two absorption peaks; one at 680 nm and the other around 430 nm [120]. The light absorption behavior of each accessory pigment differs from that of another. The overall absorption spectrum of the pigments shows lowest absorption in the green-yellow region. The process of light harvesting involves light absorption by antenna pigments, which get excited and transfer energy to successive elements in the array via resonance energy transfer and finally to the reaction center. The oxygen evolution via water splitting takes place at PS II; the electrons generated by this process pass through PS II and PS I to help in the synthesis of the reductant NADPH (reduced nicotinamide adenine dinucleotide), needed for carbon fixation [121].

The process of photosynthesis is generally explained by the modified Z-scheme [122-127]. P_{680} in PS II absorbs light and goes to an excited state. It releases an electron to a primary acceptor named pheophytin. P^{+}_{680} thus formed receives electrons successively from a

manganese cluster that is a part of a water-oxidizing complex. The water splitting reaction,

$$2H_2O \rightarrow O_2+4H^+ + 4e^- \quad (2.4.2)$$

is mediated by a redox-active tyrosine residue [127,128]. The electrons are transferred to the manganese ions and protons are released into the lumen. The electron transferred to pheophytin moves to plastoquinone Q_A, then to polypeptide bound plastoquinone Q_B and to a cytochrome b_6f complex containing the cytochrome f and b, iron-sulfur cluster and quinone. From this complex, the electron is transferred to plastocyanin (PC), see **Fig. 2.9**. The electron is now available for the processes in PS I. P_{700} in PS I also goes to the excited state by receiving light energy. It transfers an electron to the chlorophyll primary electron acceptor A_0 and receives an electron from plastocyanin. The electron transfer takes place from A_0 to the phylloquinone secondary electron acceptor A_1 [129,130], then to an iron-sulfur center and to Ferredoxin (Fd) [131]. Ferredoxin provides an electron for the reduction of $NADP^+$ (oxidized nicotinamide adenine dinucleotide) that combines with a proton in the stroma to form NADPH. The reaction is catalyzed by the flavoenzyme, ferredoxin-NADP oxidoreductase (FNR) [129,132]. A process called photophosphorylation takes place in parallel to the electron transport process across the thylakoid membrane. The electron transport leads to the creation of a proton gradient across the thylakoid membrane. The electrochemical energy from this proton gradient drives the synthesis of ATP (adenosine triphosphate) from ADP (adenosine diphosphate) enzyme and inorganic phosphate [133]. In some species a cyclic transport of electrons takes place in PS I that lead to the synthesis of ATP instead of NADPH, a process that does not require water oxidation [134].

The light independent reactions take place in the stroma with the help of ATP and NADPH. In a process called the Calvin-Benson cycle, or carbon fixation, carbon dioxide from the atmosphere is captured and converted into carbohydrates [135]. The reaction is catalyzed by the enzyme RuBisCO (ribulose-1,5-biphosphate

carboxylase/oxygenase). The overall photosynthesis process can be represented as

$$H_2O + CO_2 + \text{light} \rightarrow CH_2O + O_2 \quad (2.4.3)$$

As discussed above, although water is split in green plants no molecular hydrogen evolution takes place. A study conducted by Jackon and Ellms in 1896 showed that hydrogen was evolved by a filamentous cyanobacterium *Anabaena* [136]. The basic research in the field started in 1920s with bacterial hydrogen production. Studies showed that both eucaryotic and prokaryotic types of microalgae can generate hydrogen under certain conditions. In 1942, Gaffron and Rubin, in a study using green algae *Scenedesmus Obliquus*, observed that if the organism was allowed to adapt to a dark anaerobic condition for a certain period it would produce hydrogen the rate of which becomes dramatically higher when illuminated after this adaptation period [137]. This discovery did not receive much attention till the 1970s, co-incident with the Arab oil embargo and correlated interest in developing hydrogen from renewable sources. The basic difference between photosynthesis and biophotolysis processes is that in photosynthesis ferredoxin reduces NADP to NADPH with the addition of a proton that is used by RUBisCO for carbohydrate preparation with the help of carbon dioxide, whereas in biophotolysis ferredoxin activates certain enzymes that produce molecular hydrogen [138,138]. The focus of biophotolysis research has generally been on microalgae, both green algae (eucaryote) and cyanobacteria or blue-green algae (prokaryote) that possess enzymes capable of acting as catalysts for the photo assisted production of hydrogen. Microalgae have the highest photosynthetic capability per unit volume [140], and grow much faster than higher-level plants and with minimum nutrition requirements.

The unique hydrogen production ability of green algae and cyanobacteria is due to the presence of certain enzymes that are absent in other plant species in which only CO_2 reduction takes place. These enzymes, named hydrogenase and nitrogenase, catalyze molecular hydrogen production. Green algae possess the hydrogenase enzyme, whereas cyanobacteria species can have both nitrogenase and hydrogenase enzymes. Two types of hydrogenase enzymes are active in the hydrogen production process: the

reversible or classical hydrogenase, and membrane bound uptake hydrogenase [141]. The reversible hydrogenase oxidizes ferredoxin, or other low redox electron carriers, in a readily reversible reaction. The normal function of membrane bound uptake hydrogenase is to derive reductant from hydrogen; this enzyme does not produce hydrogen in measurable amounts. The normal function of nitrogenase in cyanobacteria is to convert nitrogen to ammonia [142,143], but it can also drive a hydrogen production reaction in the absence of nitrogen.

Hydrogenase was named by Stephenson and Stickland in 1931, discovered in their experiments using anaerobic colon bacterium Escherichia Coli that evolved hydrogen [144-146]. Hydrogenase enzymes are metalloproteins that contain sulfur and nickel and/or iron [147]. To date over 80 hydrogenase enzymes have been identified. These enzymes reversibly catalyze hydrogen production/uptake reactions:

$$2H^+ + e^- \leftrightarrow H_2 \tag{2.4.4}$$

However, these enzymes favor either a forward (hydrogen evolution) or a backward (hydrogen uptake) reaction depending upon their redox partners provided by the host organism [148]. The reactions take place at a catalytically active region buried in the protein. These core regions access or release hydrogen through continuous hydrophobic channels connecting the surface and the active core region of the enzyme structural unit.

Depending upon the metal composition at the active sites, the hydrogenase enzymes are of three types: [Fe] hydrogenase, [NiFe] hydrogenase, and metal free or [FeS] cluster-free hydrogenase [149-152]. There is another type called [NiFeSe] hydrogenase, which is usually included in the [NiFe] hydrogenase family. Among the categories, [Fe] hydrogenase has the highest activity for hydrogen synthesis from protons and electrons [151]. This is the reversible hydrogenase present in green algae that generates hydrogen via biophotolysis [153]. The catalytically active core unit, called 'H cluster', consists of a six-iron cluster with a two-iron (binuclear iron) subcluster bound to carbon monoxide (CO) and cyanide (CN^-) ligands [154-157]. The binuclear iron subcluster is unique to [Fe]

hydrogenase and promotes oxygen dependent hydrogen uptake; hence oxygen inhibits the hydrogen evolution activity of the [Fe] hydrogenase. [NiFe] hydrogenase is the most abundant type of hydrogenase. These are found in conjunction with nitrogenases in cyanobacteria as well as other nitrogen-fixing prokaryotes [158]. The active unit, the H-cluster, in [NiFe] hydrogenase has a heterodinuclear active site with cysteine thiolates bridging a nickel ion with an iron center [159-161]. This enzyme generally promotes the hydrogen uptake reaction. Cyanobacteria possess both uptake and bi-directional hydrogenase [162]. The metal-free or [FeS] cluster free hydrogenase was discovered in the 1990s within methanogenic bacteria [163-165]. This type of hydrogenase does not contain iron or nickel at the active site but contains iron in the inactive region [165]. This enzyme catalyzes the reversible reduction of N^5, N^{10}-methenyltetrahydromethanopterin with H_2 to N^5, N^{10}-methylene-tetrahydromethanopterin [148]; the turn over number for hydrogenase enzyme approaches 10^6 per second.

Nitrogenase enzyme is a two-component protein system, consisting of dinitrogenase and a nitrogenase reductase, that uses the nitrogen and energy of ATP to produce ammonia and hydrogen [143,166]. The nitrogen fixation reaction is accompanied by the production of hydrogen as a side reaction the rate of which is about one-fourth that of the nitrogen fixation. In the nitrogen free ambient, the nitrogenase enzyme functions like a hydrogenase and metabolizes the photosynthetically generated reductants to molecular H_2 [167]. The production of hydrogen by nitrogenase is unidirectional as a byproduct in contrast with that by hydrogenase. The overall reaction can be given as

$$N_2 + 8H^+ + 8e^- + 16ATP \rightarrow 2NH_3 + H_2 + 16ADP + 16P_i \qquad (2.4.5)$$

where P_i represents inorganic phosphate.

Depending upon the metal content at the active site, there are three categories of nitrogenase enzymes which are named as MoFe, VFe and Fe nitrogenase [168,169]. The most common among these is MoFe nitrogenase. The two components in the MoFe nitrogenase protein system are the dinitrogenase (MoFe protein or protein I) and the dinitrogenase reductase (Fe protein or protein II) [162]. The

protein II component in all the three categories are similar, whereas the molybdenum in protein I is replaced by vanadium and iron to form VFe and Fe nitrogenases respectively [169]. Although nitrogenases are sensitive to oxygen cyanobacteria have the inherent ability to protect it from oxygen evolution spatially or temporally. Nitrogenase catalyzed by hydrogen production is highly energy intensive due to the consumption of 16ATP. Hence these are less efficient compared to the hydrogenase-based reaction; the turn over number is less than 10 per second.

In general there are two routes, discussed below, in which hydrogen production can be accomplished using the noted enzymes in combination with sunlight and water. One route is called direct biophotolysis, in which hydrogen production can be considered a single-step water splitting reaction. The other route is called indirect biophotolysis, in which intermediate steps are involved in the process but the overall reaction gives hydrogen and oxygen from water [170,171].

Direct Biophotolysis

Direct biophotolysis is the biological process in which water is split into hydrogen and oxygen without involvement of intermediates; water is the electron donor in the process, and the energy that drives the process is obtained from visible radiation. The electron transfer route is the same as that in the case of NADPH formation (the Z-scheme discussed earlier) during photosynthesis with the exception that ferredoxin transfers electrons to the hydrogenase enzyme which in turn reduces protons to form molecular hydrogen. The hydrogenase catalyzed hydrogen production process in green algae is schematically represented in **Fig. 2.9**.

Under anaerobic conditions with a low partial pressure of hydrogen and under low intensity illumination, hydrogen evolution takes place and the overall reaction can be represented by (2.4.1) [172]; the electron transfer route is as follows [141]:

$$\begin{array}{l} H_2O \rightarrow PSII \rightarrow PSI \rightarrow Ferredoxin \rightarrow Hydrogenase \rightarrow H_2 \\ \downarrow \\ O_2 \end{array}$$

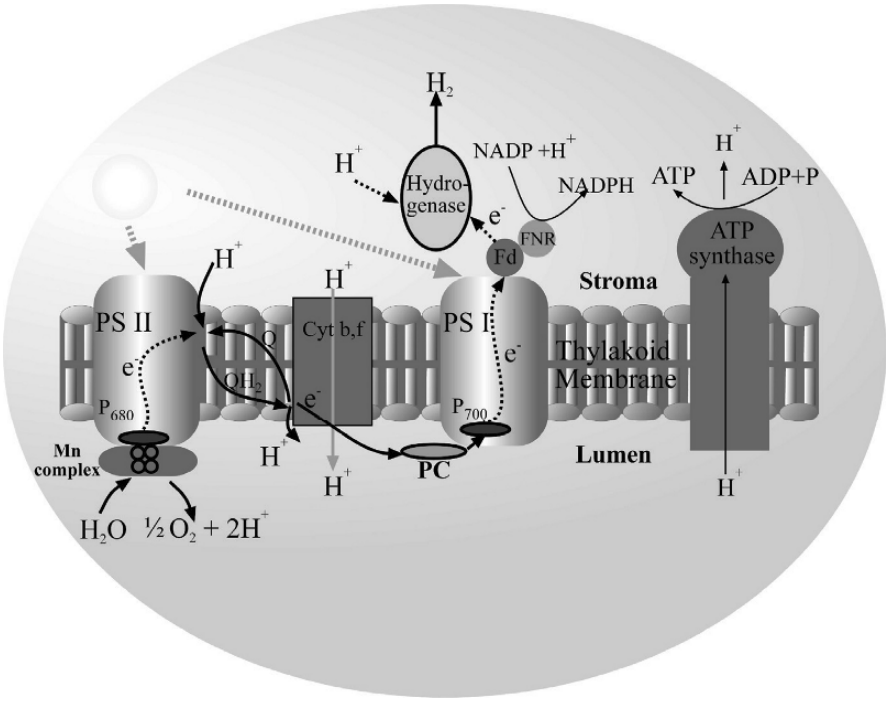

Fig. 2.9: Hydrogenase mediated hydrogen production process in green algae. See the text for abbreviations.

The energetics of electron transfer with the help of photoexcitated chlorophyll in PSII and PSI is shown in **Fig. 2.10**. Electrons from water can be considered traversing through PS I and PS II to Ferredoxin and then to hydrogenase, while protons are released to the lumen (**Fig. 2.9**). The energy from the absorbed light enables electron transport from water, at a potential of ~ +0.82 V, to ferredoxin at a potential of -0.44 V [142]. As indicated in **Fig. 2.9** two photons are responsible for transport of a single electron across the thylakoid membrane. Hence four electrons and eight photons are needed for the formation of a single hydrogen molecule. The need for such a number of electrons and photons is one of the factors that limit the maximum possible efficiency of hydrogen production through this process.

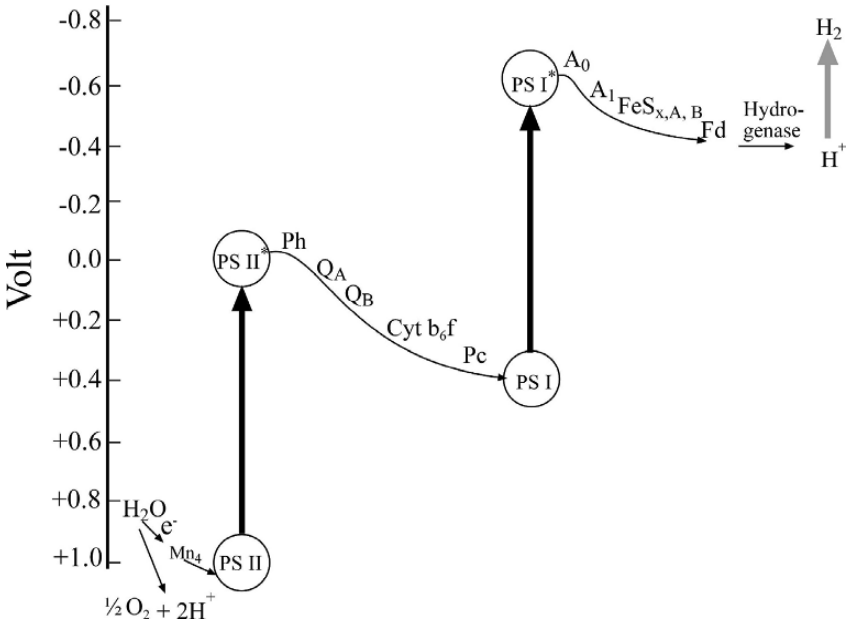

Fig. 2.10: Energetics of electron transfer in direct biophotolysis.

A necessary condition for hydrogen production is that the hydrogenase enzyme should be activated by exposure of the biophotolysis algal species to a dark, anaerobic condition for a period ranging from a few minutes to several hours depending upon the algal strain. In this condition the algal species activates hydrogenase to produce a small amount of hydrogen then used as a reductant for carbon dioxide. When exposed to light, again in anaerobic conditions, the hydrogen production resumes but at a much higher rate through the photosynthetic process. The process of hydrogen production creates a sustained flow of electrons across the thylakoid membrane that promotes the synthesis of ATP using protons [173].

Green alga evolve hydrogen through direct biophotolysis as they contain reversible hydrogenase [Fe hydrogenase]. Apart from *Scenedesmus obliquust* that was used by Gaffron and Rubin [137], green algae species including *Chlamydomonas reinhardtii* and *Chlamydomonas moewusii* have also proven useful [122,141,174]. Among these a maximum efficiency of hydrogen production has

been observed in *Chlamydomonas reinhardii*. Several mutants of these species have been studied for extending the process to a commercial scale. While most studies have been performed using fresh water green algae, there are a few studies investigating the use of marine green algae [140,175,176].

The reversible hydrogenase responsible for the hydrogen evolution in these species is known for its oxygen sensitivity. The presence of oxygen (say, >0.1%) impairs the electron transport through ferredoxin and hydrogenase in turn inhibiting hydrogen evolution [177]. During their initial work, Gaffron and Rubin found that hydrogen evolution stops some time after exposing the species to light [137]; in the presence of light normal photosynthesis starts with the release of oxygen, inhibiting hydrogen evolution. Hence, sustained hydrogen generation by hydrogenase requires removal of the evolved oxygen.

Various methods have been sought for the sustained, continuous production of hydrogen via direct biophotolysis. Flushing the bioreactor continuously with an inert gas to remove the oxygen has proven to be one method; Greenbaum continuously purged a bioreactor with argon to remove the evolved oxygen thereby sustaining hydrogen production for several hours [178]. Although this method has been used in laboratory settings by several groups, scale-up of the bio-reactor for practical applications is difficult due to the needed inert gas flow rates, and the low partial pressure of the hydrogen produced [177]. Oxygen scavengers or absorbers have also been employed, but have yet to be found economically feasible; for example, glucose and glucose oxidase have both been found useful for facilitating sustained hydrogen production [179]. An approach of perhaps greater utility is the use of mutants exhibiting high oxygen tolerance [180]. However none of these techniques have yet found use in commercial scale hydrogen production.

Indirect Biophotolysis

As the name implies indirect biophotolysis involves more than one step, with the net effect being water splitting. Indirect biophotolysis can be effectively performed using either hydrogenase or

nitrogenase, hence both green algae and cyanobacteria can be utilized. In this section, our discussion is limited to processes catalyzed by nitrogenase in cyanobacteria.

As a way of intrinsically protecting its nitrogen fixing enzyme, nitrogenase, from oxygen different cyanobacteria strains either spatially or temporally separate the oxygen evolving photosynthetic process from the nitrogen fixing process [179]. Carbohydrate preparation via photosynthesis takes place in one step, and nitrogenase-catalyzed nitrogen fixation occurs by consuming this carbohydrate in the second step. If provided with reductant and ATP in anaerobic and nitrogen deficient conditions nitrogenase switches its function to hydrogen production. Carbohydrate synthesis, assisted by carbon dioxide intake, act as an intermediate step between water oxidation and hydrogen evolution. Under illumination in anaerobic conditions this accumulated carbohydrate is used by nitrogenase to produce hydrogen. The overall effect is that water is consumed and oxygen and hydrogen are released whereas carbon dioxide is recycled. The reactions can be represented as [173]

$$CO_2+H_2O \rightarrow CH_2O + O_2 \quad (2.4.6)$$
$$CH_2O + H_2O \rightarrow CO_2 +2H_2 \quad (2.4.7)$$

With the net reaction

$$2H_2O \rightarrow 2H_2 + O_2 \quad (2.4.8)$$

At 25°C and 1 bar the enthalpy change (ΔH) involved in reactions (2.3.5) and (2.3.6) is, respectively, 211.5 kJ and 361 kJ, hence that of reaction (2.3.7) is 572.5 kJ [173]; four ATP are consumed per nitrogen molecule fixed or hydrogen molecule evolved. Even in the presence of nitrogen, 25% of the ATP used is for hydrogen evolution. The whole process requires twenty photons and hence indirect biophotolysis using nitrogenase is not as energetically efficient as direct biophotolysis. A typical nitrogenase based hydrogen production process via indirect biophotolysis process is illustrated in **Fig. 2.11**.

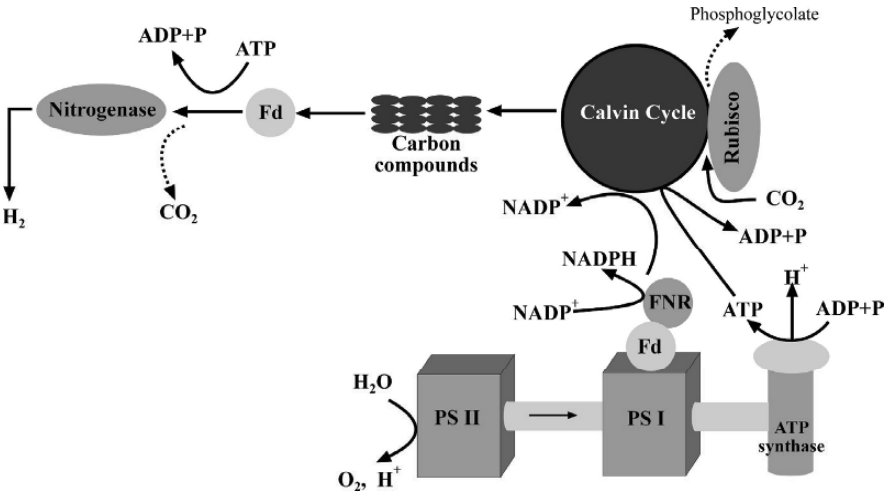

Fig. 2.11: Nitrogenase mediated indirect biophotolysis process in cyanobacteria.

Heterocystous cyanobacteria, which are filamentous blue-green algae, spatially separate the oxygen and nitrogen fixing (or hydrogen evolving) processes [181,141]. Heterocystous cyanobacteria possess two types of cells, vegetative cells and heterocysts. Photosynthesis and oxygen evolution take place in vegetative cells, which contain PS I and PS II; nitrogen fixation or hydrogen evolution takes place in the heterocysts. Heterocyst cells have thick walls with an envelope composed of a glycolipid layer and a polysaccharide layer [182]. This wall acts as an oxygen diffusion barrier and helps to maintain an anaerobic environment in the heterocysts. Further, these cells exhibit high respiration rates absorbing any residual oxygen [179]. The carbohydrate produced in the vegetative cells via photosynthesis is transferred to the heterocysts where it is used for nitrogen fixing or hydrogen evolution. Thus oxygen and hydrogen evolution can simultaneously take place in such species. A scheme of hydrogen evolution by heterocystous cyanobacteria is shown in **Fig. 2.11** [141].

$H_2O \rightarrow$ photosystems (vegetative cells) $\rightarrow [CH_2O]_2 \rightarrow$ Ferredoxin $\rightarrow$ Nitrogenase

$\downarrow$ $\uparrow$ $\downarrow$ NAPDH $\downarrow$

O_2 CO_2 recycle CO_2 H_2

Some of the heterocystous cyanobacteria strains used for hydrogen evolution include *Anabaena Azollae, Anabaena variabilis, Anabaena cylindrica, Nostoc muscorum, Nostoc spongiaeforme,* and *Westiellopsis prolifica* [174]. In the early 1970s Beneman and co-workers demonstrated that hydrogen and oxygen could be produced simultaneously for several hours using *Anabaena cylindrica* in a nitrogen deficient atmosphere [183,184] by flowing inert gas. In this process simultaneous oxygen and hydrogen evolution takes place, hence a gas separation step is required.

Some strains like unicellular and non-heterocystous filamentous diazotrophic cyanobacteria separate the oxygen and hydrogen evolution steps temporally [185]. Periods of O_2 evolution and CO_2 fixation alternate with periods of N_2 fixation or H_2 production [179], with the latter process taking place in an anaerobic environment. In many cases oxygen evolution occurs under illumination and nitrogen fixation (or hydrogen evolution) occurs in the dark [185], while carbohydrate accumulation occurs during the first phase and its consumption occurs in the second. The hydrogen evolution scheme by non-heterocystous cyanobacteria is given below [141]:

$$
\begin{array}{lllll}
H_2O \rightarrow \text{photosystems (vegetative cells)} \rightarrow [CH_2O]_2 \rightarrow \text{Ferredoxin} \rightarrow & & & & \text{Nitrogenase} \\
\downarrow & & \uparrow & \downarrow \text{NAPDH} & \text{or hydrogenase} \\
O_2 & & CO_2 \text{ recycle} & CO_2 & \uparrow \quad \downarrow \\
 & & & \text{PS-I} \rightarrow \text{ATP} & H_2
\end{array}
$$

Some of the unicellular strains used for hydrogen evolution include *Plectonema boryanum, Oscillotoria Miami BG7, Oscillotoria limnetica, Synechococcus sp., Aphanothece halophytico, Mastidocladus laminosus,* and *Phormidium valderianum*. A fundamental advantage in using these strains is that there is no need of separating hydrogen and oxygen as these are evolved under different conditions at different times.

Cyanobacteria, in general, carry the three enzymes related to hydrogen production; nitrogenase, reversible hydrogenase, and uptake hydrogenase [186]. The presence and amount of these enzymes vary from strain to strain and according to the growth conditions. Uptake hydrogenase ionizes hydrogen produced by nitrogenase during nitrogen fixation so as to use the protons for the

next cycle. The combined effect of the enzymes determines the overall hydrogen evolution rate by the cyanobacteria. For a high rate of hydrogen evolution the contribution from uptake hydrogenase should be reduced. As the turn over number of nitrogenase is about one-thousandth of that of hydrogenase, for the purposes of hydrogen production the strains with higher activity of reversible hydrogenase should be chosen [177]. Efforts have been made to reduce the activity of uptake hydrogenase, and enhance that of nitrogenase and reversible hydrogenase by manipulation of the metabolic scheme [174]. Uptake hydrogenase deficient strains were found to be useful for providing a higher hydrogen evolution rate [187].

Selective mutation and molecular cloning techniques have been used for developing strains useful for hydrogen production rather than nitrogen fixation [179]. For example, a mutant strain of Anabaena (AMC 414) in which the large subunit of the uptake hydrogenase (hupL) was inactivated by a deletion event, produced H_2 at a rate that was more than twice that of the parent strain, Anabaena PCC 7120 [187]. Asada and Kawamura reported on aerobic hydrogen production using an uptake hydrogenase deficient *Anabaena sp*. strain N7363 [188].

An advantage of using cyanobacteria is that it can be grown with minimal nutritional requirements, while fish can consume the waste bodies keeping environmental impact to a minimum [179]. Although the nitrogenase of the bacteria is not immediately useful for hydrogen production due to its low turnover number, the thermodynamic driving force (obtained from ATP) allows the enzyme to generate hydrogen against elevated pressures, up to about 50 atmospheres [173]. This is in contrast with direct photoelectrolysis where hydrogen can be produced only near normal atmospheric pressures.

Two-stage Indirect Biophotolysis

The process of growing organisms and utilizing them for hydrogen production in a single bioreactor, either by direct biophotolysis or nitrogenase based indirect biophotolysis, has several limitations; these processes require huge bioroeactors for specie growth, the simultaneous production of oxygen and hydrogen necessitates a

separation step, and oxygen evolution may within a short span of time inhibit hydrogen production. Historically, it was realized early-on that such problems could hinder any possibility of large-scale production of hydrogen. Hence hydrogenase based indirect biophotolysis processes involving two or more stages, using either green algae or cyanobacteria, were developed [170]. In general, a two-stage process consists of growing microalgae, either green algae or cyanobacteria, in open ponds with their transfer to an enclosed photobioreactor where hydrogen evolution takes place [179,189]. In a two-stage indirect biophotolysis process conceptualized by Benemann [179], the algal growth takes place at first in open ponds where carbohydrates are prepared by carbon dioxide reduction and stored in the cells. The culture is then transferred to a dark anaerobic fermentation vessel in which activation of hydrogenase takes place with evolution of a small amount of hydrogen; the biomass is then illuminated, under anaerobic conditions, to produce hydrogen [179]. The three processes can be represented as

Carbohydrate storage:

$$\begin{array}{ccccccccc} O_2 & & & & & & CO_2 & & \\ \uparrow & & & & & & \downarrow & & \\ H_2O & \rightarrow & PSII & \rightarrow & PSI & \rightarrow & Ferredoxin & \rightarrow & RUBISCO \rightarrow [CHO] \end{array}$$

Dark fermentation and formation of low amounts of hydrogen:

$$\begin{array}{ccccccc} CO_2 & & & & & & \\ \uparrow & & & & & & \\ [CHO] & \rightarrow & Ferredoxin & \rightarrow & Hydrogenase & \rightarrow & H_2 \end{array}$$

Light driven hydrogen evolution:

$$\begin{array}{ccccccc} CO_2 & & & & & & \\ \uparrow & & & & & & \\ [CHO] & \rightarrow & PSI & \rightarrow & Ferredoxin & \rightarrow & hydrogenase \rightarrow H_2 \end{array}$$

The overall effect is the decomposition of water. An advantage of this method is that only a low light energy input, about one quantum/H_2, is required for hydrogen evolution [179]. During

illumination, a low activity of PSII is required to avoid simultaneous oxygen evolution, either by use of low light intensity, dense cultures, or inhibitors.

Melis and co-workers [177,190-192] observed that sulfur deprived cultures can inhibit simultaneous photosynthetic oxygen production and hence sustain hydrogen evolution. Sulfur deprived *C. reinhardtii* cultures kept in a sealed environment partially inactivate the function of photosystem II [193], hence the photosynthetic oxygen evolution rate drops below the rate of respiratory oxygen consumption leading to an intercellular anaerobiosis. In such conditions the algal cells maintain a low level of respiratory activity and start generating hydrogen from stored carbohydrates; continuous hydrogen production under illumination up to about 70 hours has been observed [173,177,193]. Kosourov and co-workers sustained hydrogen production for more than 140 hours by the re-addition of sulfur [194], as needed, obtaining a maximum yield of 6.6 mmol of hydrogen per hour per liter of culture; the *C. reinhardtii* culture-containing cell was illuminated (300 $\mu E/m^2/s$; μE = microEinsteins) on both sides by fluorescent lamps. Guan and co-workers grew marine green algae *P. subcordiformis* in sea water, then transferred the culture for sulfur deprivation where it was subjected to a dark anaerobic incubation period of 32 hours for hydrogenase activation before illuminating (160 $\mu E/m^2/s$) them for hydrogen production [195]. The hydrogen evolution was sustained for about ten hours with a peak evolution rate of 0.00162 mmol/per liter of culture/hour obtained after 2.5 hours of illumination.

Major Challenges

Both direct and indirect biophotolysis routes suffer from a number of challenges that currently prohibit them from becoming commercially viable processes [180]; these include, but are not limited to, solar energy conversion efficiency and the difficulty of bioreactor design. In particular the low solar energy to hydrogen conversion efficiency is a matter of major concern in the field of biophotolysis. The efficiency is calculated as [180,172]:

$$\varepsilon = \frac{\text{Hydrogen production rate} \times \text{Hydrogen energy content}}{\text{Light energy input}} \qquad (2.4.9)$$

Microalgae utilize radiation for hydrogen production only in the wavelength region 400-700 nm; this is known as the photosynthetically active radiation (PAR). Only about 43% of the solar radiation falls in the PAR wavelength region. In some cases efficiency has been calculated using only the energy falling in the PAR region, with efficiency values reaching about 22% [196]. However, when commercial applications are considered in comparison to other means of producing hydrogen it is more appropriate to consider total solar energy input in the denominator of equation (2.4.9); as such calculations show a maximum solar conversion efficiency of 11% is possible with biophotolysis. However considering the amount of light reflected at different surfaces, and the low number of photons converted into hydrogen, upper values realistically practical are about 6-9% [197,198].

A major reason for this low efficiency is the light saturation effect in microalgae. The conversion efficiency of algae reaches a maximum value at low light intensities [180,199,200], typically at 10 to 20% of the maximum intensity, with the remaining portion of the energy wasted as heat or fluorescence [199]. This is due to the presence of a large number of antenna molecules per reaction center that collects photons in excess of that can be utilized by the photosystems for electron transfer across the thylakoid membrane [189]. A reduction in the number of antenna pigments per reaction center by genetic or metabolic means has been suggested as a solution to this problem; algal mutants with a reduced number of antennae pigments have been found to have saturations occurring at higher light intensities.

It is of course important to harvest as much light as possible to reduce needed bioreactor areas. Lower efficiencies mean greater land requirements for the collection of enough solar energy for meaningful amounts of hydrogen production. The annual average solar irradiance reaching earth is approximately 210 W/m^2. For an optimistic conversion efficiency of 10%, conversion of solar energy to hydrogen by biophotolysis equates to an energy equivalent of 5.5 US gallons of gasoline (121.8 MJ/gallon) per square meter of insolation, per year. In 2002 the United States used 135.4 billion gallons of gasoline; to satisfy this energy demand using 10% efficient biophotolysis (the above figures), would necessitate a

square of land approximately 100 miles (157 km) by 100 miles (157 km) [173,187,194,210]. This amount of land, while large, appears a modest commitment in comparison to various consequences of continued fossil fuel use. Optimization of light intensity, pH, temperature and nutrient content while maintaining low partial pressures of H_2 and CO_2 are necessary to improve the hydrogen production rate. Additionally, the purity of the hydrogen produced is critical for its commercial use, particularly in fuel cells. Depending upon the technique used, the produced hydrogen may contain water vapor, oxygen, carbon dioxide, and various organic species. We note that 50%w/w potassium hydroxide has been used as a carbon dioxide absorbent, and an alkaline pyragallol solution for removing oxygen; the evolved gases would need to be passed through a dryer or condensation unit to remove moisture.

There are different types of reactor geometries used for hydrogen production through biological processes, such as flat panel and vertical column reactors, and it is necessary to properly design and maintain the photobioreactor appropriate for the technique used [139,180,202-204]. Safety is of paramount interest in designing the bioreactors, particularly if oxygen and hydrogen are simultaneously produced. There are as yet un-solved difficulties involving the transfer out of the reactor the hydrogen produced under water by the algae. In addition fouling of the bioreactor by unwanted species will quite possibly be a significant issue for continuously running reactors. Also reactor efficiency could be reduced by self-shadowing if proper attention is not given to the distribution of the biomass throughout the bioreactor [167].

2.5 Other Techniques for H_2 production via Water Splitting

In addition to the three major techniques discussed above other methods, that we now briefly consider, have been studied for hydrogen production via water splitting.

2.5.1 Hydrogen Production by Mechano-catalytic Water Splitting

In 1998 Domen and co-workers reported evolution of hydrogen and oxygen from distilled water when certain oxide powders were

dispersed in it and then agitated using a magnetic stirrer [205]. Their experiments showed that these gases were generated according to the stoichiometric composition of water when a material like NiO, Co_3O_4, Cu_2O, Fe_2O_3, AWO_4 (A=Fe,Co,Ni,Cu) or $CuMO_2$ (M=Al, Fe, Ga) was used and that indeed the process was water splitting [206-210]. Rubbing of the particles by the stirring rod against the bottom wall of the reaction vessel apparently had a key role in the process. It is believed that the electric charges created due to frictional forces together with catalytic activity of the oxide powder is responsible for the water splitting. Hence the phenomenon was named mechano-catalytic water splitting. In the process the conversion of energy takes place from mechanical to electrical and finally to chemical energy.

A typical experimental set up consists of a flat-bottomed pyrex glass cell that has provisions for evacuation and circulation of the evolved gases. In their experiments, the group generally used 200 ml of distilled water and 0.1 g of the desired oxide powder kept suspended by stirring [206]. The cell is initially evacuated prior to the reaction; the evolution rate of hydrogen and oxygen reduces when the over-head pressure increases due to the evolved gases, hence the cell needs to be periodically evacuated. The rate of evolved gases increases with stirring speed, saturating above 1500 rpm. Various means of stirring have been considered, with the shape, size and material of the stirring mechanism as well as reaction vessel material having an influence on the reaction and hence hydrogen and oxygen evolution rates. Pyrex glass was found superior to vessels made of quartz, sapphire, polytetrafluorethylene (PTFE) and alumina for driving the reaction, while a Teflon coated stirring rod was found highly appropriate for the reactions.

A hydrogen evolution rate of about 35 μmol/hr over the first few hours of reaction using NiO powder was reported. This decreased with time reaching a value of 20 μmol/h after 55 hours. The energy efficiency was calculated using the equation [206]

$$\varepsilon = (E_c/E_i)x100$$

where E_c is the maximum useful work output that can be obtained from evolved hydrogen and E_i the mechanical energy input. An

efficiency of up to 4.3% was obtained depending upon the shape and size of the stirring rod.

The stoichiometric evolution of hydrogen and oxygen was observed only on using the previously mentioned oxides. From the mass of the powder measured before and after the reaction, it was concluded that these materials are not undergoing any changes but acting only as a catalyst, hence the hydrogen and oxygen production was attributed to water splitting. Interestingly, oxides such as CuO, FeO, Fe_2O_3 and CoO evolved very small amounts of hydrogen without detectable evolution of oxygen, and photocatalytic materials like TiO_2, ZnO and WO_3 did not produce any gases. The results from a large number of oxides are given [206,209].

The group that discovered this technique tried to explain the phenomena based on triboelectricity [206]. According to this hypothesis, the friction between the particles and bottom of the vessel leads to charge separation, with the powder taking a negative charge and the reaction vessel becoming positively charged, with the triboelectric generated charges driving the redox reactions resulting in water splitting. However, their findings and conclusions were challenged by various researchers [211,212]; alternate explanations put forth included some kind of auto-redox reactions between water and oxides, electrical charging of the powders due to friction followed by local discharge as well as thermal decomposition due to friction induced localized increase in temperature (up to about 5000 K). To date there has been no consensus on the actual mechanism [213].

Tokio Ohta proposed a theory that explained several of the experimental findings [214], based on the observation that the oxides that showed mechano-catalytic water splitting are p-type semiconductors having an excess amount of oxygen, and that the surface of glass is susceptible to form micro cracks due to frictional rubbing [215]. According to the theory, friction between the stirring rod (R) and bottom of the glass cell (G) in the presence of the particles creates a number of micro-crevices on the surface of G [215-217]. The crevices have a high density of dangling bonds that accept electrons from R. Thus a frictional electrical capacitor is formed between the rod and glass. The coating (Teflon) on the magnetic stirrer, reaction vessel and distilled water are non-

conductors, making formation of the frictional electrical capacitor possible. When the oxide particles trapped in the micro-crevices are contacted by R they are subject to high electric fields. The excess oxygen in the interstitials of the p-type oxide semiconductor receives electrons from neighboring metal ions and become O^- (or O^{2-}), with a positive hole getting associated with this metal ion. The insulator coating on the stirring rod R gets positively charged due to the loss of electrons by friction.

The electrons and holes thus created are responsible for water splitting; R acts as the anode and G acts as the cathode. When R comes into contact with the particle the O^- at the particle surface transfers electrons to the positively charged surface of R. These electrons are eventually transferred to G due to rubbing action. The positive holes associated with metal ions proceed via a hopping mechanism through successive metal ions in the particle toward the negatively charged G. The holes reach the surface of the particle where it encounters the potential barrier due to work-function difference. If the barrier height is not sufficiently low, tunneling of the holes could take place. This happens when the potential barrier is steep and the barrier height at the Fermi level is in the order of the wavelength associated with the carrier. These holes oxidize water and oxygen is evolved. The reaction is

$$2h^+ + H_2O \rightarrow 2H^+ + ½\ O_2$$

The protons move towards the bottom of the glass cell G where they combine with electrons to generate hydrogen gas. Another possibility is the transfer of electrons from the particle surfaces to water, so that hydrogen is evolved according to the reaction [218]

$$2e^- + 2H_2O \rightarrow 2OH^- + H_2$$

OH^- combines with the positive charge at the stirring rod R to evolve oxygen. The reaction is

$$2OH^- + R^{n+} \rightarrow H_2O + ½\ O_2 + R^{+(n-2)}$$

At the same time holes created in the process hop through the particles finally combining with negative charge at the glass surface (G).

Ohta simplified the nomenclature and named the process as mechanolysis [214]. The theory puts restrictions on the particle size, which should match with the crevices and hence it should be between 1 to 10 μm. Although mechano-catalytic water splitting is simple and does not involve any toxic materials, a major limitation is the low yield of hydrogen. Most of the work in this technique was done between 1998 and 2000; no new results based on this technique have been seen since. It does seem an intriguing way to capture the energy of ocean waves, with reaction chambers left to tumble in the ocean surf.

2.5.2 Hydrogen Production by Water Plasmolysis

Electric discharge plasma technology is well developed and plays a crucial role in many industrial processes. In electrical discharges within gaseous media, the electrical energy is mainly transformed into electron kinetic energy, with the highly energetic electrons ionizing gas molecules/atoms by inelastic collisions sustaining the discharge. Within plasma various processes take place including ionization, dissociation and excitation of molecules and/or atoms. Hence discharge plasma processes are highly useful in carrying out thermodynamically non-spontaneous reactions ($\Delta G > 0$) such as water splitting, as well as hydrogen production by splitting methane and other hydrocarbons.

Plasmolysis involves the process of water splitting using electrical discharges. The plasma in general is classified as *cold plasma*, which includes glow discharge plasma or non-equilibrium plasma, or *hot plasma* created by electrical arcs. In both processes the electron temperatures in the plasma can reach several tens of thousands of degrees. In general, the process involves spraying water into or passing water vapor through a plasma created in a reactor and collecting the reaction products including hydrogen at the output. In water splitting using glow discharge plasma, a major portion of the energy is expended for vibrational excitation and dissociative attachment. The magnitude and nature of interaction between electrons and molecules depends upon the electron energy

and electron energy distribution function. Depending upon the plasma conditions a number of species such as H_2O* (excited molecule), H, OH, H^-, H^+, H_2O_2, H_2 etc. can be found in the plasma. In order to increase the yield of hydrogen production certain reactions have to be favored and others inhibited. For example, OH radicals can combine with H_2 to form H and H_2O and hence it reduces the hydrogen yield. Catalysts are normally used to suppress unfavorable reactions and to selectively activate certain bonds [219-221]. Carbon dioxide is one such catalyst, reducing the OH free radical concentration and hence back reactions [222]. Such catalysts mitigate the need of having a high degree of ionization of water molecules for obtaining higher yields [223].

Chen and co-workers reported on water splitting conducted in a tubular reactor at atmospheric pressure using plasma and catalyst integrated technologies (PACT) [224,225]. The tubular PACT reactor consisted of a quartz tube fitted with an outer electrode, and an inner electrode passing through the center of the tube. The inner electrode was coated with a catalytic material like Ni, Pd, Rh or Au and the outer electrode was made of aluminum foil. Plasma was created in the quartz tube using a low frequency (8.1 kHz) electric field applied between the electrodes. Argon bubbled through water was used as the feed gas, containing 2.3 mol% water. Maximum hydrogen production was achieved using gold catalyst. At a voltage of about 2.5 kV, 14.2% of the water in the feed was converted into hydrogen (0.32 mol% H_2).

The energy conversion efficiency was calculated as

$$\varepsilon = (R_H \Delta G/P) \times 100$$

where R_H is the rate of hydrogen production and P is the input power. Chen and co-workers have reported efficiencies up to 2.09%. The possible reactions in the plasma can be given as

$$H_2O + Ar^* \rightarrow H_2O^* + Ar$$
$$H_2O^* \rightarrow HO\cdot + H\cdot$$
$$HO\cdot + Ar^* \rightarrow H\cdot + O\cdot + Ar$$
$$2H\cdot \rightarrow H_2$$
$$2O\cdot \rightarrow O_2$$

The oxygen radicals get adsorbed on the catalyst surfaces and either combine to form oxygen or react with metal surfaces. This favors the decomposition reaction of H_2O and enhances the hydrogen yield. To date the hydrogen yield and efficiencies are not high enough for practical application.

2.5.3 Hydrogen Production by Water Magnetolysis

Magnetolysis is electrolysis but with the needed voltage created inside the electrolyzer by magnetic induction. The idea was suggested by Bockris and Gutmann in 1985 to eliminate the technical problems in supplying the low voltage, high current needed for electrolyzers [223]. An electrolyzer unit with a parallel configuration of individual cells operates at voltages between 1.5 V to 2.0 V dc requiring currents of several hundred amperes. Satisfying these electrical requirements requires transformers and rectifiers giving rise to higher capital expenditures, as well as losses in electrical energy. Hence, the idea was to generate the needed low voltage and high current directly inside the electrolyte via magnetic induction using a homopolar generator.

In a configuration used by Ghoroghchian and Bockris [226], a stainless steel disc of 30.48 cm diameter and 0.31 cm thickness was connected to a bearing isolated shaft; the disk was mounted vertically in an electrolytic cell containing a 35% potassium hydroxide electrolyte. The whole assembly was placed within a magnetic field, generated by an electromagnet, and the disk rotated using an electric motor. Hence a potential difference was created across the disk with the center acting as the anode and the rim as the cathode. Under a magnetic field of 0.86 T and at 2100 rpm, a potential difference of 2 V was created that resulted in hydrogen generation via electrolysis. The disk in such a configuration suffers viscous drag. To overcome this difficulty the magnetic field strength should be as large as possible, or the electrolyte should also be rotated so as to avoid any relative movement between the disk and the electrolyte. It was estimated that for producing hydrogen at minimum power consumption a magnetic field greater than 11 T is required [223].

The advances made over the past several decades to improve the performance of electronic circuitry, e.g. rectifiers, have made electrolyzers increasingly commercially viable. Furthermore in advanced electrolyzers a series cell configuration is used (bipolar filter press, SPE, *etc*.) and hence there is no need to work in low voltage high current mode with its inherent I^2R electrical losses. Consequently, the dormant magnetolysis field stands a good chance of remaining dormant.

2.5.4 Hydrogen Production by Water Radiolysis

Radiolysis of water involves the use of radioactive materials and/or highly energetic particles for water decomposition. The energy for dissociation can be obtained from γ rays or high-energy neutrons or charged particles like α and ß. Radiolysis of water has been known for over a century and is of considerable importance in nuclear reactor design where water is used as a coolant. Particles and radiation from the reactor core can decompose coolant water into hydrogen peroxide and oxygen, in addition to hydrogen, giving rise to corrosion problems. The technique received much attention when it was first used as a means to produce hydrogen in the 1950s [227] as means to effectively utilize nuclear waste emissions.

When water is irradiated by emissions from radioactive materials, a number of reactions leading to the production of a variety of species take place depending upon the nature and energy of the radiation. As the high-energy particles/radiations traverse the water they lose energy and eject electrons from the atomic shells. These high-energy electrons create low energy secondary electrons and help to initiate further reactions. Some of the prominent species formed as a result are H_2, H_2O_2, OH, H, HO_2, O and O_2 [228-230].

The effectiveness of interaction between a given type of radiation and water in yielding a particular species is represented by parameter G, the radiochemical or radiological yield. It is defined as the number of species created per unit of deposited energy (usually 100 eV is considered as the unit). It depends upon the energy transfer to the medium, called linear energy transfer (LET), from a given type of radiation [231]. The G value is about 0.45 for hydrogen when γ radiation is used. That is, 0.45 molecules of H_2 are

produced per 100 eV energy absorbed by liquid water when a γ ray is passed through it. The yield is higher when energetic particles are used, with a value close to 1 when pure water is irradiated at room temperature [232]. The radiolysis of pure steam performed using Cm-244 alpha-particles gave a yield of 8 molecules/100 eV at 300°C whereas the yield was only 2 molecules/100 eV at 250°C [233]. With fast neutrons Sunaryo and co-workers reported a G value of 1.5 at 250°C [230]. The hydrogen yield is limited by back reactions between H_2 and OH.

Although the G value for hydrogen when pure water is irradiated by γ radiation is low, studies indicate that irradiation of water in the presence of solid materials improves the yield [234]. Irradiation of water adsorbed on solid oxides, mainly use of porous silica and zeolites have been studied, appreciably increases the yield [233,235-239]. Nakashima and Masaki obtained yields close to 1.5 molecules/100eV when water adsorbed zeolytes (Type Y) were irradiated using ^{60}Co γ-rays at room temperature [238]. LaVerne and Tandon reported on irradiating water adsorbed on micron-sized particles of CeO_2 and ZrO_2 with γ radiation (dose rate 202 Gy/min) or 5 MeV α particles [239]. The yield was found greater for ZrO_2, with the yield dramatically increasing when the number of adsorbed layers of water was limited to one or two; they obtained 150 molecules/100eV when ZrO_2 having two layers of water molecules was irradiated with γ rays. However, this yield was calculated using the energy adsorbed by the water layers alone and not using the total energy absorbed by both oxide and water. Cecal and co-workers [233], from their study using oxides such as ZrO_2, TiO_2, BeO or SiO_2 dispersed in water, found that yield was highest for ZrO_2. Caer and co-workers also studied the effect of pore size on yield by irradiating nanoporous SiO_2 with 1-MeV electrons [240]; an increase in yield with reduction in pore size was observed. In general, electrons and holes formed inside the oxide that then migrate to the surface are believed responsible for the water splitting [235].

Radiolysis of water is, at least for today, inherently limited due to the use of radioactive materials by which the product stream could be contaminated by radioactive species. Consequently while

of scientific interest this technique is not considered to have the potential to compete with other major water splitting techniques.

References

1. Funk JE (2001) Thermochemical hydrogen production: past and present. Int J Hydrogen Energy 26:185–190
2. Sato S (1979) Thermochemical hydrogen production. In: Ohta T (ed) Solar hydrogen energy systems. Pergamon Press, New York
3. Ihara S (1979) Direct thermal decomposition of water. In: Ohta T (ed) Solar hydrogen energy systems. Pergamon press, New York
4. Casper MS (1978) Hydrogen manufacture by electrolysis, thermal decomposition and unusual techniques. Noyes Data Corporation, New Jersey, USA
5. Kreuter W, Hofmann H (1998) Electrolysis: the important energy transformer in a world of sustainable energy. Int J Hydrogen Energy 23:661–666
6. Ewan BCR, Allen RWK (2005) A figure of merit assessment of the routes to hydrogen. Int J Hydrogen Energy 30:809–819
7. Divisek J (1990) Water electrolysis in a low and medium temperature regime. In: Wendt H (ed) Electrochemical hydrogen technologies - Electrochemical production and combustion of hydrogen. Elsevier, New York, pp 137–212
8. Donitz W, Erdle E, Streicher R (1990) High temperature electrochemical technology for hydrogen production and power generation. In: Wendt H (ed.) Electrochemical hydrogen technologies - Electrochemical production and combustion of hydrogen. Elsevier, New York, pp 213–259
9. Barbir F (2005) PEM electrolysis for production of hydrogen from renewable energy sources. Sol Energy 78:661-669
10. JANAF (1971) Thermochemical tables QD511.D614
11. Rossmeisl J, Logadottir A, Norskov JK (2005) Electrolysis of water on (oxidized) metal surface. Chem Phys 319:178–184

12. Takahashi T (1979) Water electrolysis. In:Solar hydrogen energy systems. Ohta T (ed.) Pergamon Press, New York
13. Burstein GT (2005) A hundred years of Tafel's equation: 1905-2005. Corrosion Sci 47:2858–2870
14. Esaki H, Nambu T, Morinaga M, Udaka M, Kawasaki K (1996) Development of low hydrogen overpotential electrodes utilizing metal ultra-fine particles. Int J Hydrogen Energy 21:877–881
15. Nagai N, Takeuchi M, Kimura T, Oka T (2003) Existence of optimum space between electrodes on hydrogen production by water electrolysis. Int J Hydrogen Energy 28:35–41
16. de Jonge RM, Barendrecht E, Janssen LJJ, van Stralen SJD (1982) Gas bubble behavior and electrolyte resistance during water electrolysis. Int J Hydrogen Energy 7:883–894
17. Sillen CWMP, Barendrecht E, Janssen LJJ, van Stralen SJD (1982) Gas bubble behavior during electrolysis. Int J Hydrogen Energy 7:577–587
18. Roy A, Watson S, Infield D (2006) Comparison of electrical energy efficiency of atmospheric and high-pressure electrolyzers, Int J Hydrogen Energy 31:1964–1979
19. Dickson EM, Ryan, JW, Smulyan MH (1977) The hydrogen energy economy: a realistic appraisal of prospects and impacts. Praeger, New York, USA.
20. Ulleberg O (2003) Modeling of advanced alkaline electrolyzers: a system simulation approach. Int J Hydrogen Energy 28:21–33
21. Wendt H, Imarisio G (1988) Nine years of research and development on advanced water electrolysis. A review of research program of the commission of the European communities. J Applied Electrochem 18:1–14
22. Dutta S (1990) Technology assessment of advanced electrolytic hydrogen production. Int J Hydrogen Energy 15:379–386
23. LeRoy RL (1983) Industrial water electrolysis: Present and future, Int J Hydrogen Energy. 8:401–417

24. LeRoy RL, Bowen CT, LeRoy DJ (1980) The thermodynamics of aqueous water electrolysis. J Electrochem Soc 127:1954–1962
25. Onda K, Kyakuno T, Hattori K, Ito K (2004) Prediction of production power for high-pressure hydrogen by high-pressure water electrolysis. J Power Sources 132:64–70
26. Chen L, Lasia A (1991) Study of the kinetics of hydrogen evolution reaction on nickel-zinc Alloy electrodes. J Electrochem Soc 138:3321–3328
27. Rosalbino F, Maccio D, Angelini E, Saccone A, Delfino S (2005) Electrocatalytic properties of Fe-R (R=rare earth metal) crystalline alloys as hydrogen electrodes in alkaline water electrolysis. J Alloys Compd 403:275–282
28. Bockris JOM (1956) Kinetics of activation controlled consecutive electrochemical reactions: anodic evolution of oxygen. J Chem Phys 24:817–827
29. Chapman EA (1965) Production of hydrogen by electrolysis. Chem Process Eng 46:387–393
30. Dutta S (1990) Technology assessment of advanced electrolytic hydrogen production. Int J Hydrogen Energy 15:379–386
31. Yazici B, Tatli G, Galip H, Erbil M (1995) Investigation of suitable cathodes for the production of hydrogen gas by electrolysis. Int J Hydrogen Energy 20:957-965
32. Suffredini HB, Cerne JL, Crnkovic FC, Machado SAS, Avaca LA (2000) Recent developments in electrode materials for water electrolysis. Int J Hydrogen Energy 25:415–423
33. Nagarale RK, Gohil GS, Shahi VK (2006) Recent developments on ion-exchange membranes and electro-membrane processes. Adv Colloid Interface Sci 119:97–130
34. Singh RN, Pandey JP, Anitha KL (1993) Preparation of electrodeposited thin films of Nickel-Iron alloys on mild steel for alkaline water electrolysis. Part I: Studies on oxygen evolution. Int J Hydrogen Energy 18:467–473
35. Kaninski MPM, Stojic DLJ, Saponjic DP, Potkonjak NI, Miljanic SS (2006) Comparison of different electrode

materials- Energy requirements in the electrolytic hydrogen evolution process. J Power Sources 157:758-764
36. Hu W, Cao X, Wang F, Zhang Y (1997) Short Communication: a novel cathode for alkaline water electrolysis. Int J Hydrogen Energy 22:621–623
37. Stojic DL, Maksic AD, Kaninski MPM, Cekic BD, Mijanic SS (2005) Improved energy efficiency of the electrolytic evolution of hydrogen - Comparison of conventional and advanced electrode materials. J Power Sources 145:278–281
38. Raney M (1925), U.S. patent 1563787; (1927) 1628191; (1933) 1915473. From E. Endoh E et al. (1987) New Raney nickel electrode. Int. J. Hydrogen Energy 12:473–47939
39. Singh SP, Singh RN, Poillearat G, Chartier P (1995) Physiochemical and electrochemical characterization of active films of $LaNiO_3$ for use as anode in alkaline water electrolysis. Int J Hydrogen Energy 20:203–210
40. Rosa VM, Santos MBF, da Silva EP (1995) New materials for water electrolysis diaphragms. Int J Hydrogen Energy 20:697–700
41. http://americanhistory.si.edu/fuelcells/pem/pemmain.htm
42. http://www.chemsoc.org/chembytes/ezine/2000/kingston_jun00. htm
43. Han SD, Park KB, Rana R, Singh KC (2002) Developments of water electrolysis technology by solid polymer electrolyte. Ind J Chem 41A:245–253
44. Hijikata T (2002) Research and development of international clean energy network using hydrogen energy (WE-NET). Int J Hydrogen Energy 27:115–129
45. Paddison SJ (2003) Proton conduction mechanism at low degrees of hydration in sulfonic acid-based polymer electrolyte membranes. Ann Rev Mater Res 33:289–319
46. Rasten E, Hagen G, Tunold R (2003) Electrocatalysts in water electrolysis with solid polymer electrolyte. Electrochimica acta 48:3945–3952
47. Linkous CA, Anderson HR, Kopitzke RW, Nelson GL (1998) Development of new proton exchange membrane

electrolytes for water electrolysis at higher temperatures. Int J Hydrogen Energy 23:525–529
48. Linkous CA (1993) Development of solid polymer electrolytes for water electrolysis at intermediate temperatures. Int J Hydrogen Energy 18:641–646
49. Grigoriev SA, Porembsky VI, Fateev VN (2006) Pure hydrogen production by PEM electrolysis for hydrogen energy. Int J Hydrogen Energy 31:171–175
50. Millet P, Andolfatto F, Durand R (1996) Design and performance of a solid polymer electrolyte water electrolyzer. Int J Hydrogen Energy 21:87–93
51. Herring JS, Brien JEO, Stoots CM, Hawkes GL, Hartvigsen JJ, Shagnam M (2007) Progress in high temperature electrolysis for hydrogen production using planar SOFC technology. Int J Hydrogen Energy 32:440–450
52. Hino R, Haga K, Aita H, Sekita K (2004) R&D on hydrogen production by high temperature electrolysis of steam. Nucl Eng Des 233:363–375
53. Dutta S, Morehouse JH, Khan JA (1977) Numerical analysis of laminar flow and heat transfer in a high temperature electrolyzer. Int J Hydrogen Energy 22:883–895
54. Donitz W, Erdle E (1985) High temperature electrolysis of water vapor-status of development and perspectives for application. Int J Hydrogen Energy 10:291–295
55. Yildiz B, Kazimi MS (2006) Efficiency of hydrogen production systems using alternative nuclear energy technologies. Int J Hydrogen Energy 31:77-92
56. Kharton VV, Marques FMB, Atkinson A (2004) Transport properties of solid oxide electrolyte ceramics: a brief review. Solid State Ionics 174:135–149
57. Hong HS, Chae US, Choo ST, Lee KS (2006) Microstructure and electrical conductivity of Ni/YSZ and NiO/YSZ composites for high temperature electrolysis prepared by mechanical alloying. J Power Sources 149:84-89
58. Utgikar V, Thiesen T (2006) Life cycle assessment of high temperature electrolysis for hydrogen production via nuclear energy. Int J Hydrogen Energy 31:939–944

59. Liepa MA, Borhan A (1986) High-temperature steam electrolysis: Technical and economic evaluation of alternative process designs. Int J Hydrogen Energy 11:435
60. Funk JE, Reinstrom RM (1966) Energy requirements in the production of hydrogen from water. Ind Eng Chem Process Des Dev 5:336-342
61. Funk JE (1976) Thermochemical production of hydrogen via multistage water splitting processes, Int J Hydrogen Energy 1:33–43
62. Engels H, Funk JE, Hesselmann K, Knoche KF (1987) Thermochemical Hydrogen-Production. Int J Hydrogen Energy 12:291–295
63. Rosen MA (1996) Thermodynamic comparison of hydrogen production processes. Int J Hydrogen Energy 21:349–365
64. Scott DS (2003) Exergy. Int J Hydrogen Energy 28:369–375
65. Struck BD, Schutz GH, Van Velzen D, (1990) Cathodic hydrogen evolution in thermochemical-electrochemical hybrid cycles. In: electrochemical hydrogen technologies-Electrochemical production and combustion of hydrogen Wendt H (ed), Elsevier, New York, pp 213-259
66. Schultz K, Herring S, Lewis M, Summers WA (2005) The hydrogen reaction. Nucl Eng Int 50:10–15
67. Abanades S, Charvin P, Flamant G, Neveu P (2006) Screening of water-splitting thermochemical cycles potentially attractive for hydrogen production by concentrated solar energy. Energy 31:2805–2822
68. Perkins C, Weimer AW (2004) Likely near-term solar-thermal water splitting technologies. Int J Hydrogen Energy 29:1587–1599
69. Yildiz B Kazimi MS (2006) Efficiency of hydrogen production systems using alternative nuclear energy technologies. Int J Hydrogen Energy 31:77–92
70. Kodama T (2003) High temperature solar chemistry for converting solar heat to chemical fuels. Prog Energy & Combust. Sci 29 567–597
71. Steinfeld A (2005) Solar thermochemical production of hydrogen – a review. Sol Energy 78:603–615

72. Kalogirou SA (2004) Solar thermal collectors and applications. Prog Energy Combust Sci 30:231–295
73. Sakurai M, Bilgen E, Tsutsumi A, Yoshida K (1996) Solar UT-3 thermochemical cycle for hydrogen production. Sol Energy 57:51-58
74. Baykara SZ (2004) Hydrogen production by direct solar thermal decomposition of water, possibilities for improvement of process efficiency. Int J Hydrogen Energy 29:1451–1458
75. Baykara SZ (2004) Experimental solar water thermolysis. Int J Hydrogen Energy 29:1459–1469
76. Lede J, Lapicque F, Villermaux J (1983) Production of hydrogen by direct thermal decomposition of water. Int J Hydrogen Energy 8:675–679
77. Kogan A, Spiegler E, Wolfshtein M (2000) Direct solar thermal splitting of water and on-site separation of the products. III. Improvement of reactor efficiency by steam entrainment. Int J Hydrogen Energy 25:739–745
78. Fletcher EA (2001) Solar thermal processing: A Review. J Solar Energy Eng 123:63–74
79. Kogan A (1998) Direct thermal splitting of water and on-site separation of the products—II. Experimental feasibility study. Int J Hydrogen Energy 23:89–98
80. Nakamura T (1977) Hydrogen production from water utilizing solar heat at high temperatures. Sol Energy 19:467–475
81. Ross RT (1966) Thermodynamic limitations on the conversion of radiant energy into work. J Chem Phys 45:1–7
82. Kogan A (1998) Direct thermal splitting of water and on-site separation of the products—II. Experimental feasibility study. Int J Hydrogen Energy 23:89–98
83. Sturzenegger M, Ganz J, Nuesch P, Schelling T (1999) Solar hydrogen from a manganese oxide based thermochemical cycle. J PhyS. IV:JP 9:3–331
84. Kaneko H, Gokon N, Hasegawa N, Tamaura Y (2005) Solar thermochemical process for hydrogen production using ferrites. Energy 30:2171–2178

85. Kodama Y, Kondoh Y, Yamamoto R, Andou H, Satou N (2005) Thermochemical hydrogen production by a redox system of ZrO_2-supported Co(II)-ferrite. Sol Energy 78:623–631
86. Alvani C, Ennas G, La Barbera A, Marongiu G, Padella F, Varsano F (2005) Synthesis and characterization of nanocrystalline $MnFe_2O_4$: advances in thermochemical water splitting. Int J Hydrogen Energy 30:1407–1411
87. Kodoma T, Kondoh Y, Kiyama A, Shimizu K (2003) Hydrogen production by solar thermochemical water-splitting/methane-reforming process. International Solar Energy Conference pp 121–128
88. Lede J, Ricart EE, Ferrer M (2001) Solar thermal splitting of zinc oxide: A review of some of the rate controlling factors. J Solar Energy Eng 123:91–97
89. Agrafiotis C, Roeb M, Konstandopoulos AG, Nalbandian L, Zaspalis VT, Sattler C, Stobbe P, Steele AM (2005) Solar water splitting for hydrogen production with monolithic reactors. Sol Energy 79:409–421
90. Wegner K, Ly HC, Weiss RJ, Pratsinis SE, Steinfeld A (2006) In situ formation and hydrolysis of Zn nanoparticles for H_2 production by the 2-step ZnO/Zn water-splitting thermochemical cycle. Int J Hydrogen Energy 31:55–61
91. Steinfeld A (2002) Solar hydrogen production via a two-step water-splitting thermochemical cycle based on Zn/ZnO redox reactions. Int J Hydrogen Energy 27:611–619
92. Haueter P, Moeller S, Palumbo R, Steinfeld A (1999) The production of zinc by thermal dissociation of zinc oxide-solar chemical reactor design. Sol Energy 67:161–167
93. Berman A, Epstein M (2000) The kinetics of hydrogen production in the oxidation of liquid zinc with water vapor. Int J Hydrogen Energy 25:957–967
94. Perret R, Chen Y, Besenbruch G, Diver R, Weimer A, Lewandowski A, Miller E (2005) High-temperature thermochemical: solar hydrogen generation research. DOE Hydrogen Program Progress Report

95. Yalcin S (1989) A review of nuclear hydrogen production. Int J Hydrogen Energy 14:551–561
96. Huang CP, Raissi AT (2005) Analysis of sulfur-iodine thermochemical cycle for solar hydrogen production. Part I: decomposition of sulfuric acid. Sol Energy 78:632–646
97. Beghi GE (1981) Review of thermochemical hydrogen production. Int J Hydrogen Energy 6:555–566
98. Norman JH, Mysels KJ, Sharp R, Williamson D (1982) Studies of the sulfur-iodine thermochemical water-splitting cycle. Int J Hydrogen Energy 7:545–556
99. Keefe DO, Allen C, Besenbruch G, Brown L, Norman J, Sharp R (1982) Preliminary results from bench-scale testing of a sulfur-iodine thermochemical water splitting cycle. Int J Hydrogen Energy 7:381–392
100. Kasahara S, Hwang GJ, Nakajima H, Choi HS, Onuki K, Nomura M (2003) Effects of chemical engineering parameters of the IS process on total thermal efficiency to produce hydrogen from water. J Chem Eng Jpn 36:887–899
101. Onuki K, Inagaki Y, Hino R, Tachibana Y (2005) Research and development on nuclear hydrogen production using HTGR at JAERI. Prog Nucl Energy 47:496–503
102. Kubo S, Kasahara S, Okuda H, Terada A, Tanaka N, Inaba Y, Ohashi H, Inagaki Y, Onuki K, Hino R (2004) A pilot test plan of the thermochemical water-splitting iodine-sulfur process. Nucl Eng Des 233:355–362
103. Kubo S, Nakajima, Kasahara HS, Higashi S, Masaki T, Abe H, Onuki (2004) A demonstration study on a closed-cycle hydrogen production by the thermochemical water-splitting iodine-sulfur process. Nucl Eng Des 233:347–354
104. Huang CP, Raissi AT (2005) Analysis of sulfur-iodine thermochemical cycle for solar hydrogen production. Part I: decomposition of sulfuric acid. Sol Energy 78:632–646
105. Gorensek MB, Summers WA, Buckner MR (2004) Model-based evaluation of thermochemical nuclear hydrogen processes, Trans Am Nucl Soc 91:107–108
106. Sakurai M, Miyake N, Tsutsumi A, Yoshida K (1996) Analysis of a reaction mechanism in the UT-3

thermochemical hydrogen production cycle. Int J Hydrogen Energy 21:871–875
107. Sakurai M, Bilgen E, Tsutsumi A, Yoshida K (1996) Adiabatic UT-3 thermochemical process for hydrogen production. Int J Hydrogen Energy 21:865–870
108. Teo ED, Brandon NP, Vos E, Kramer GJ (2005) A critical pathway energy efficiency analysis of the thermochemical UT-3 cycle, Int J Hydrogen Energy 30:559–564
109. Lemort F, Lafon C, Dedryvere R, Gonbeau D (2006) Physicochemical and thermodynamic investigation of the UT-3 hydrogen production cycle: a new technological assessment. Int J Hydrogen Energy 31:906–918
110. Tadokoro Y, Kajiyama T, Yamaguchi T, Sakai N, Kameyama H, Yoshida K (1997) Technical evaluation of UT-3 thermochemical hydrogen production process for an industrial scale plant. Int J Hydrogen Energy 22:49–56.
111. Lewis MA, Serban M, Basco JK (2004) A progress report on the chemistry of the low temperature Cu-Cl thermochemical cycle. Trans Am Nucl Soc 91:113–114
112. Dokiya M, Kotera Y (1976) Hybrid cycle with electrolysis using Cu-Cl system. Int J Hydrogen Energy 1:117-121
113. Deneuve F, Roncato JP (1981) Thermochemical or hybrid cycles of hydrogen production- technolo-echonomical comparison with water electrolysis. Int J Hydrogen Energy 6:9-23
114. Beghi GE (1985) Development of thermochemical and hybrid processes for hydrogen production. Int J Hydrogen Energy 10:431-438
115. Deneuve F, Roncato JP (1981) Thermochemical or hybrid cycles of hydrogen production- technico-economical comparison with water electrolysis. Int J Hydrogen Energy 6:9-23
116. Summers WA, Buckner MR (2005) Hybrid sulfur thermochemical process development, DOE Hydrogen Program Progress Report
117. Carty R, Cox K, Funk J, Soliman M, Conger W (1977) Process sensitivity studies of the Westinghouse sulfur cycle

for hydrogen generation, International journal of hydrogen energy 2:17-22
118. Bilgen E (1988) Solar hydrogen production by hybrid thermochemical processes, Solar Energy 41:199-206
119. Volkov AG, Volkova-Gugeshashvili MI, Brown-McGauley CL, Osei AJ (2007) Nanodevices in nature: electrochemical aspects. Electrochim Acta 52:2905–2912
120. Volkov AG (1989) Oxygen evolution in the course of photosynthesis: molecular mechanisms. Bioelectrochem Bioenergetics 21:3–24
121. Giardi MT, Pace E (2005) Photosynthetic proteins for technological applications. Trends Biotechnol 23:257–263
122. Weaver PF, Lien S, Seibert M (1980) Photobiological production of hydrogen. Sol Energy 24:3–45
123. Prince RC (1996) Photynthesis: the Z-scheme revised. TIBS:121–122
124. Kramer DM, Avenson TJ, Edwards GE (2004) Dynamic flexibility in the light reactions of photosynthesis governed by both electron and proton transfer reactions. Trends Plant Sci 9:349–357
125. Bukhov NG (2004) Dynamic light regulation of photosynthesis (A review). Russ J Plant physiol 51:742–753
126. Howell JM, Vieth WR (1982) Biophotolytic membranes: simplified kinetic model of photosynthetic electron transport, J Mol Catal 16:245–298
127. Renger G (2001) Photosynthetic water oxidation to molecular oxygen: apparatus and mechanism, Biochim Biophys Acta 1503:210–228
128. Kraub N (2003) Mechanisms for photosystems I and II. Curr Op Chem Biol 7:540–550
129. Fromme P, Jordan P, Kraub N (2001) β Structure of photosystem I. Biochim Biophys Acta 1507:5-31
130. Fairclough WV, Forsyth A, Evans MCW, Rigby SEJ, Purton S, Heathcote P (2003) Bidirectional electron transfer in photosystem I: electron transfer on the PsaA side is not essential for phototrophic growth in *Chlamydomonas*. Biochim Biophys Acta 1606:43–55

131. Setif P (2001) Ferredoxin and flavodoxin reduction by photosystem I. Biochim Biophys Acta 1507:161–179
132. Onda Y, Hase T (2004) FAD assembly and thylakoid membrane binding of ferredoxin: $NADP^+$ oxidoreductase in chloroplasts. FEBS Lett 564:116–120
133. Reeves SG, Hall DO (1978) Photophosphorylation in chlorplasts. Biochim Biophys Acta 463:275–297
134. Joliot P, Joliot A (2006) Cyclic electron flow in C3 plants. Biochim Biophys Acta 1757:362–368
135. Griffin KL, Seemann JR (1996) Plants, CO_2 and photosynthesis in the 21st century. Chem Biol 3:245–254
136. Jackson DD, Ellms JW (1896) On odors and tastes of surface waters with special reference to *Anabaena*, a microscopial organism found in certain water supplies of Massachusetts, Report of the Massachusetts State Board Health 410–420
137. Gaffron H, Rubin J (1942) Fermentative and photochemical production of hydrogen in algae. J Gen Physiol 219–240
138. Kruse O, Rupprecht J, Mussgnug JH, Dismukes GC, Hankamer B (2005) Photosynthesis: a blueprint for solar energy capture and biohydrogen production technologies, Photochem Photobiol Sci 4:957–969
139. Rupprecht J, Hankamer B, Mussgnug JH, Ananyev G, Dismukes C, Kruse O (2006) Perspectives and advances of biological H_2 production in microorganisms. Appl Microbiol Biotechnol 72:442–449
140. Miura Y (1995) Hydrogen-Production by Biophotolysis Based on Microalgal Photosynthesis. Process Biochem 30:1–7
141. Das D, Veziroğlu TN (2001) Hydrogen production by biological processes: a survey of literature. Int J Hydrogen Energy 26:13–28
142. Rao KK, Hall DO (1984) Photosynthetic production of fuels and chemicals in immobilized systems. Trends Biotechnol. 2:124–129
143. Howard JB, Rees DC (1996) Structural basis of biological nitrogen fixation. Chem Rev 96:2955–2982

144. Adams MWW (1990) The structure and mechanism of iron-hydrogenases. Biochim Biophys Acta 1020:115–145
145. Adams MWW, Mortenson LE, Chen JS (1981) Hydrogenase, Biochim Biophys Acta 594:105-176
146. Krasna AI (1979) Hydrogenase: properties and applications, Enzyme Microb. Technol. 1:165-172
147. Darensbourg MY, Lyon EJ, Smee JJ (2000) The bio-organometallic chemistry of active site iron in hydrogenases. Coord Chem Rev 206-207:533–561
148. Vignais PM, Billoud B, Meyer J (2001) Classification and phylogeny of hydrogenases. FEMS Microbiol Rev 25:455–501
149. Mertens R, Liese A (2004) Biotechnological applications of hydrogenases, Curr Op Biotechnol 15:343–348
150. Das D, Dutta T, Nath K, Kotay SM, Das AK, Veziroglu TN (2006) Role of Fe-hydrogenase in biological hydrogen production. Curr Sci 90:1627–1637
151. Happe T, Hemeschemeier A, Winkler M, Kaminski A (2002) Hydrogenases in green algae: do they save the algae's life and solve our energy problems? Trends Plant Sci 7:246–250
152. Frey M (2002) Hydrogenases: Hydrogen-activating enzymes. Chem Biochem 3:153–160
153. Happe T, Kaminski A (2002) Differential regulation of the Fe-hydrogenase during anaerobic adaptation in the green algae Clamydomonas reinhardtii. Eur J Biochem 269:1022–1032
154. Adams MWW, Stiefel EI (1998) Biological hydrogen production: Not so elementary, Science 282:1842–1843
155. Thauer RK, Klein AR, Hartmann GC (1996) Reactions with molecular hydrogen in microorganisms: evidence for a purely organic hydrogenation catalyst. Chem Rev 96:3031–3042
156. Ma Y, Balbuena PB (2007) Density functional theory approach for improving the catalytic activity of a biomimetic model based on the Fe-only hydrogenase active site. J Electroanal Chem (in press)

157. Nicolet Y, Lemon BJ, Fontecilla-Camps JC, Peters JW (2000) A novel FeS cluster in Fe-only hydrogenases. TIBS 25:138–143
158. Appel J, Schulz R (1998) Hydrogen metabolism in organisms with oxygenic photosynthesis: hydrogenases as important regulatory devices for a proper redox poising. J Photochem Photobiol 47:1–11
159. Bauwman E, Reedijk J (2005) Structural and functional models related to the nickel hydrogenases. Coord Chem Rev 249:1555–1581
160. Volbeda A, Charon MH, Piras C, Hatchikian EC, Frey M, Fontecilla-Camps JC (1995) Crystal structure of the nickel-iron hydrogenase from Desulfovibrio gigas. Nature 373:580–587
161. Albracht SPJ (1994) Nickel hydrogenases: in search of the active site. Biochim Biophys Acta 1188:167–204
162. Tamagnini P, Axelsson R, Lindberg P, Oxelfelt F, Wunschiers R, Lindblad P (2002) Hydrogenases and hydrogen metabolism of cyanobacteria. Microbiol Mol Biol Rev 66 (2002) 1–20
163. Korbas M, Vogt S, Meyer-Klaucke W, Bill E, Lyon EJ, Thauer RK, Shima S (2006) The iron-sulfur cluster-free hydrogenase (Hmd) is a metalloenzyme with a novel iron binding motif. J Biol Chem 281:30804–30813
164. Lyon EJ, Shima S, Burman G, Chowdhuri S, Batschauer A, Steinback K, Thauer RK (2004) UV-A/blue-light inactivation of the 'metal-free' hydrogenase (Hmd) from methanogenic archaea. Eur J Biochem 271:195–204
165. Berkessel A, Thauer RK (1995) On the mechanism of catalysis by a metal-free hydrogenase from methanogenic archaea: enzymatic transformation of H_2 without a metal and its analogy to the chemistry of alkanes in superacidic solution. Angew Chem Int Ed 34:2247
166. Rees DC, Howard JB (2000) Nitrogenase: standing at the crossroads. Curr Op Chem Biol 4:559–566
167. Asada Y Miyake J (1999) Photobiological hydrogen production. J Biosci Bioeng 88:1–6

168. Peters JW, Szilagyi RK (2006) Exploring new frontiers of nitrogenase structure and mechanism, Curr Op Chem Biol 10:101–108
169. Eady RR (2003) Current status of structure function relationships of vanadium nitrogenase, Coord Chem Rev 237:23–30
170. Benemann JR (2000) Hydrogen production by microalgae. J Appl Phycol 12 (2000) 291–300
171. Ni M, Leung DYC, Leung MKH, Sumathy K (2006) An overview of hydrogen production from biomass. Fuel Process Technol 87:461–472
172. Akkerman I, Janssen M, Rocha J, Wijffels RH (2002) Photobiological hydrogen production: photochemical efficiency and bioreactor design. Int J Hydrogen Energy 27:1195–1208
173. Prince RC, Kheshgi HD (2005) The photobiological production of hydrogen: Potential efficiency and effectiveness as a renewable fuel. Crit Rev Microbiol 31:19–31
174. Vijayaraghavan K, Soom MAM (2006) Trends in bio-hydrogen generation: A review, Environmental Sciences 3: 255-271.
175. Miura Y, Akano T, Fukatsu K, Miyasaka H, Mizoguchi T, Yagi K, Maeda I, Ikuta Y, Matsumoto H (1995) Hydrogen-Production by Photosynthetic Microorganisms. Energy Conv Manag 36:903–906
176. Miura Y, Akano T, Fukatsu K, Miyasaka H, Mizoguchi T, Yagi K, Maeda I, Ikuta Y Matsumoto H. (1997) Stably sustained hydrogen production by biophotolysis in natural day/night cycle. Energy Conv Manag 38:S533–S537
177. Hallenbeck PC, Benemann JR (2002) Biological hydrogen production; fundamental and limiting processes. Int J Hydrogen Energy 27:1185–1193
178. Greenbaum E (1980) Simultaneous photoproduction of hydrogen and oxygen by photosynthesis. Biotechnol Bioeng Symp 10:1–13

179. Benemann JR (1997) Feasibility analysis of photobiological hydrogen production. Int J Hydrogen Energy 22:979–987
180. Zaborsky OR (1998) Biohydrogen, Plenum Press, New York
181. Benemann JR, Miyamoto K, Hallenbeck PC (1980) Bioengineering aspects of biophysics. Enzyme Microb. Technol. 2:103–111
182. Adams DG (2000) Heterocyst formation in cyanobacteria. Curr Op Microbiol 3:618–624
183. Weissman JC, Benemann JR (1977) Hydrogen production by nitrogen-starved cultures of Anabaena Cylindrica. Appl Environ Microbiol 33:123–131
184. Benemann JR, Weare NM (1974) Hydrogen evolution by nitrogen-fixing Anabaena cylindrical cultures. Science 184:174–175
185. Hansel A, Linblad P (1998) Towards optimization of cyanobacteria as biotechnologically relevant producers of molecular hydrogen, a clean and renewable energy source. Appl Microbiol Biotechnol 50:153–160
186. Smith GD, Ewart GD, Tucker W (1992) Hydrogen-Production by Cyanobacteria. Int J Hydrogen Energy 17:695–698
187. Levin DB, Pitt L, Love M (2004) Biohydrogen production: prospects and limitations to practical application. Int J Hydrogen Energy 29:173–185
188. Asada Y, Kawamura S (1986) Aerobic hydrogen accumulation by a nitrogen-fixing cyanobacterium. Anabaena sp. Appl Envrion Microbiol 51:1063–1066
189. Benemann JR (1994) Photobiological Hydrogen Production. Intersociety Energy Conversion Engineering Conference Proceedings, pp. 1636–1640
190. Melis A, Zhang L, Forestier M, Ghirardi ML, Seibert M (2000) Sustained photobiological hydrogen gas production upon reversible inactivation of oxygen evolution in the green alga Chlamydomonas reinhardtii. Plant Physiol 122:127–135
191. Ghirardi ML, Zhang L, Lee JW, Flynn T, Seibert M, Greenbaum E, Melis A (2000) Microalgae: a green souce of renewable H_2. TIBTECH 18:506–511

192. Melis A (2002) Green alga hydrogen production: progress, challenges and prospects Int J Hydrogen Energy 27:1217–1228
193. Antal TK, Krendeleva TE, Laurinavichene TV, Makarova VV, Ghirardi ML, Rubin AB, Tsygankov AA, Seibert M (2003) The dependence of algal H_2 production on photosystem II and O_2 consumption activities in sulfur-deprived *Chlamydomonas reinhardtii* cells. Biochim Biophys Acta 1607:153–160
194. Kosourov S, Tsygankov A, Seibert M, Ghirardi ML (2002) Sustained hydrogen photoproduction by *Chlamydomonas reinhardtii*: effects of culture parameters. Biotechnol Bioeng 78:731–740
195. Guan YF, Deng MC, Yu XJ, Zhang W (2004) Two-stage photo-biological production of hydrogen by marine green alga Platymonas subcordiformis. Biochem Eng J,19:69–73
196. Greenbaum E (1998) Energetic efficiency of hydrogen photoevolution by algal water splitting. Biophys J 54:365–368
197. Bergene T (1996)The efficiency and physical principles of photolysis of water by microalgae Int J Hydrogen Energy 21:89–194
198. Hall DO (1978) Solar energy conversion through biology-could it be practical energy source? Fuel 57:322–333
199. Herron HA, Mauzerall D (1972) The development of photosynthesis in a greening mutant of Chlorella and an analysis of the light saturation curve. Plant physiology 50:141–148
200. Masukawa H, Mochimaru M, Sakurai H (2002) Hydrogenases and photobiological hydrogen production utilizing nitrogenase system in cyanobacteria. Int J Hydrogen Energy 27:1471-1474
201. Markov SA, Thomas AD, Bazin MJ, Hall DO (1997) Photoproduction of hydrogen by cyanobacteria under partial vacuum in batch culture or in a photobioreactor. Int J Hydrogen Energy 22:521–524

202. Modigell M, Holle N (1998) Reactor development for a biosolar hydrogen production process. Renewable Energy 14:421–426
203. Hoekema S, Bijmans M, Janssen M, Tramper J, Wijffels RH (2002) A pneumatically agitated flat-panel photobioreactor with gas re-circulation: anaerobic photoheterotrophic cultivation of a purple non-sulfur bacterium. Int J Hydrogen Energy 27:1331–1338
204. Miyake J, Miyake M, Asada Y (1999) Biotechnological hydrogen production: research for efficient light energy conversion. J Biotechnol 70:89–101
205. Ikeda S, Takata T, Kondo T, Hitoki G, Hara M, Kondo JN, Domen K, Hosono H, Kawazoe H, Tanaka A (1998) Mechano-catalytic overall water splitting, Chem Commun 2185–2186
206. Ikeda S, Takata T, Komoda M, Hara M, Kondo JN, Domen K, Tanaka A, Hosono H, Kawazoe H (1999) Mechano-catalysis-a novel method for overall water splitting. Phys Chem Chem Phys 1:4485–4491
207. Takata T, Ikeda S, Tanaka A, Hara M, Kondo JN, Domen K (2000) Mechano-catalytic overall water splitting on some oxides (II). Appl Catal A: Gen 200:255–262
208. Domen K, Ikeda S, Takata T, Tanaka A, Hara M, Kondo JN (2000) Mechano-catalytic overall water-splitting into hydrogen and oxygen on some metal oxides. Appl Energy 67:159–179
209. Hitoki G, Takata T, Ikeda S, Hara M, Kondo JN, Kakihana M, Domen K (2001) Mechano-catalytic overall water splitting on some mixed oxides. Catal Today 63:175–181
210. Hara M, Hasei H, Yashima M, Ikeda S, Takata T, Kondo JN, Domen K (2000) Mechano-catalytic overall water splitting (II) nafion-deposited Cu_2O. Appl Catal A: Gen 190:35–42
211. Ross DS (2004) Comment on "A study of Mechano-Catalysis for overall water splitting". J Phys Chem B 108:19076–19077
212. (1998) Mechano-catalytic water splitting claimed, Chemical & Engineering News 76:36

213. Hara M, Domen K (2004) Reply to "Comment on A study of mechano-catalysts for overall water splitting. J Phys Chem B 108:19078
214. Ohta T (2000) Preliminary theory of mechano-catalytic water-splitting. Int J Hydrogen Energy 25:287–293
215. Ohta T (2000) On the theory of mechano-catalytic water-splitting system. Int J Hydrogen Energy 25:911–917
216. Ohta T (2000) Mechano-catalytic water-splitting. Appl Energy 67:181–193
217. Ohta T (2000) Efficiency of mechano-catalytic water-splitting system. Int J Hydrogen Energy 25:1151–1156
218. Ohta T (2001) A note on the gas-evolution of mechano-catalytic water splitting system. Int J Hydrogen Energy 26:401
219. Suib SL, Brock SL, Marquez M, Luo J, Matsumoto H, Hayashi Y (1998) Efficient catalytic plasma activation of CO_2, NO and H_2O. J Phys Chem B 102:9661–9666
220. Luo J, Suib SL, Hayashi Y, Matsumoto H (2000) Water splitting in low-temperature AC plasmas at atmospheric pressure. Res Chem Intermed 26:849–874
221. Luo J, Suib SL, Hayashi Y, Matsumoto H (1999) Emission spectroscopic studies of plasma-induced NO decompostion and water spltting. J Phys Chem A 103 (1999) 6151–6161
222. Givotov VK, Fridman AA, Krotov MF, Krasheninnikov EG, Patrushev BI, Rusanov VD, Sholin GV (1981) Plasmochemical methods of hydrogen production, Int J Hydrogen Energy 6:441-449
223. Bockris JOM, Dandapani B, Cocke D, Ghoroghchian J (1985) On the splitting of water. Int J Hydrogen Energy 10:179–201
224. Chen X, Suib SL, Hayashi Y, Matsumoto H (2001) H_2O splitting in tubular PACT (Plasma and catalyst integrated technologies) reactors. J Catal 201:198–205
224. Kabashima H, Einaga H, Futamura S (2003) Hydrogen evolution from water, methane and methanol with nonthermal plasma. IEEE Transactions on Industry Applications 39:340–345

225. Chen X, Marquez M, Rozak J, Marun C, Luo J, Suib SL, Hayashi Y, Matsumoto H (1998) H_2O splitting in tubular plasma reactors. J Catal 178:372–377
226. Ghoroghchian J, Bockris JOM (1985) Use of a homopolar generator in hydrogen production from water. Int J Hydrogen Energy 10:101–112
227. Harteck P, Dondes S (1956) Producing chemicals with reactor radiations. Nucleonics 14:22–25
228. Daniels M, Wigg E (1966) Oxygen as a primary species in radiolysis of water. Science 153:1533–1534
229. Wojcik DS, Buxton GV (2005) On the possible role of the reaction $H^{\bullet}+H_2O \rightarrow H_2+ {}^{\bullet}OH$ in the radiolysis of water at high temperatures. Rad Phys Chem 74:210–219
230. Sunaryo GR, Katsumura Y, Ishigure K (1995) Radiolysis of water at elevated temperatures-III. Simulation of radiolytic products at 25 and 250°C under the irradiation with γ rays and fast neutrons. Rad Phys Chem 45:703–714
231. Gervais B, Beuve M, Olivera GH, Galassi ME (2006) Numerical simulation of multiple ionization and high LET effects in liquid water radiolysis, Radiation Physics and Chemistry 75:493-513
232. Katsumura Y, Sunaryo G, Hiroishi D, Ishiqure K (1998) Fast neutron radiolysis of water at elevated temperatures relevant to water chemistry. Prog Nucl Energy 32:113–121
233. Cecal A, Goanta M, Palamaru M, Stoicescu T, Popa K, Paraschivescu A, Anita V (2001) Use of some oxides in radiolytical decomposition of water. Rad Phys Chem 62:333–336
234. Sawasaki T, Tanabe T, Yoshida T, Ishida R (2003) Application of gamma radiolysis of water for H_2 production. J Radioanal Nucl Chem 255:271–274
235. Petrik NG, Alexandrov AB, Vall AI (2001) Interfacial energy transfer during gamma radiolysis of water on the surface of ZrO_2 and some other oxides. J Phys Chem B 105:5935–5944
236. Laverne JA (2005) H_2 formation from the radiolysis of liquid water with zirconia, J Phys Chem B 109:5395–5397

237. Yamamoto TA, Seino S, Katsura M, Okitsu K, Oshima R, Nagata Y (1999) Hydrogen gas evolution from alumina nanoparticles dispersed in water irradiated with gamma ray. Nanostructured Mater 12:1045
238. Nakashima M, Masaki NM (1996) Radiolytic hydrogen gas formation from water adsorbed on type Y zeolytes. Rad Phys Chem 46:241–245
239. LaVerne JA, Tandon L (2002) H_2 produced in the radiolysis of water on CeO_2 and ZrO_2. J Phys Chem B 106:380–386
240. Caer SL, Rotureau P, Brunet F, Charpentier T, Blain G, Renault JP, Mialocq JC (2005) Radiolysis of confined water: Hydrogen production at a high dose rate. Chem Phys Chem 6:2585-2596